

Original Article

Rethinking dinosaur origins: oldest known equatorial dinosaur-bearing assemblage (mid-late Carnian Popo Agie FM, Wyoming, USA)

David M. Lovelace^{1,2,*}, Aaron M. Kufner^{1,2,†}, Adam J. Fitch², Kristina Curry Rogers³, Mark Schmitz⁴, Darin M. Schwartz⁴, Amanda LeClair-Diaz⁵, Lynette St.Clair⁵, Joshua Mann⁶, Reba Teran⁷

¹Department of Geoscience, University of Wisconsin-Madison, 1215 W. Dayton St., Madison, WI 53706, United States

²University of Wisconsin-Madison, UW Geology Museum, 1215 W. Dayton St., Madison, WI 53706, United States

³Biology and Geology Departments, Macalester College, St. Paul, MN 55015, United States

⁴Department of Geosciences, Boise State University, 1910 University Drive, Boise, ID 83725, United States

⁵Fort Washakie Schools, Fremont County School District #21, 90 Ethete Road, Fort Washakie, WY 82514, United States

⁶Eastern Shoshone Tribal Historic Preservation Office, Bldg 17A, North Fork Rd., Fort Washakie, WY 82514, United States

⁷Shoshone Language Consultant, Wind River Reservation, Fort Washakie, WY 82514, United States

†These two authors contributed equally to this work.

*Corresponding author. Department of Geoscience, University of Wisconsin-Madison, 1215 W. Dayton St., Madison, WI 53706, United States. E-mail: dlovelace@wisc.edu

ABSTRACT

The origin of Dinosauria is thought to be deeply rooted in the high-latitude southern hemisphere (Gondwana). Nearly 6–10 million years separates Gondwanan faunas and the oldest known dinosaur occurrence in the northern hemisphere (Laurasia). However, our understanding of dinosaur origins is biased by an apparent absence of Carnian-aged (237–227 Mya) Laurasian terrestrial strata. Here we report on UWGM 1975/UWGM 7549, the oldest known Laurasian dinosaur *Ahvaytum bahndooiveche* gen. et sp. nov., and UWGM 7407/UWGM 7550, a silesaurid, from palaeoequatorial deposits of the lower Popo Agie Formation, Wyoming, USA. High-precision radioisotopic detrital ages [e.g. $\leq 229.04 \pm 0.24$ Mya (2σ)] from the upper Popo Agie Formation constrain an age-depth model that predicts a ~230 Mya age for UWGM 1975, making Laurasia's first unequivocal Carnian-aged sauropodomorph dinosaur comparable in age to the oldest dinosaur faunas of Gondwana. The presence of a ~230 Mya, low-latitude, early sauropodomorph from the northern hemisphere, along with a silesaurid, challenges the hypothesis of a delayed dinosaurian dispersal out of high-latitude Gondwana. These data fill a critical gap in the early record of sauropodomorph dinosaur evolution and demonstrate widespread geographic distribution by the mid-late Carnian.

Keywords: Carnian; dinosaur; Laurasia; Popo Agie Formation; Sauropodomorpha; silesaurid; Triassic

INTRODUCTION

The Carnian Epoch of the Late Triassic (237–227 Mya) (Cohen *et al.* 2013) heralded the proliferation of early dinosaurs and their closest relatives (Jones *et al.* 2013, Langer *et al.* 2018, Lee *et al.* 2018). At the same time, several prominent Early–Middle Triassic clades (e.g. rhynchosaurs, dicynodonts, and stereospondyl amphibians) underwent a significant reduction in taxonomic diversity or became extinct altogether by the earliest Norian (Dal Corso *et al.* 2020). For more than 50 years, the lack

of Carnian dinosaurs from the northern hemisphere (Laurasia) has sharply contrasted with the prevalence of the world's oldest dinosaurs in the southern hemisphere (Gondwana) (Langer *et al.* 2010, Lee *et al.* 2018, Kent and Clemmensen 2021, Novas *et al.* 2021, Griffin *et al.* 2022). Currently, the oldest known North American dinosaur, *Lepidus praecisio* Nesbitt and Ezcurra, 2015, is found in the lower Dockum Group near the classic Otis Chalk quarries of west Texas, USA, with an age no younger than the base of the Adamanian holochron (c. 221 Mya) but without

Received 12 June 2024; revised 20 September 2024; accepted 28 October 2024

[Version of Record, first published online 8 January 2025, with fixed content and layout in compliance with Art. 8.1.3.2 ICZN. <http://zoobank.org/urn:lsid:zoobank.org:pub:538C156C-5CC1-4706-8D8A-FFA6757A6590>]

© 2025 The Linnean Society of London.

This is an Open Access article distributed under the terms of the Creative Commons Attribution-NonCommercial-NoDerivs licence (<https://creativecommons.org/licenses/by-nc-nd/4.0/>), which permits non-commercial reproduction and distribution of the work, in any medium, provided the original work is not altered or transformed in any way, and that the work is properly cited. For commercial re-use, please contact reprints@oup.com for reprints and translation rights for reprints. All other permissions can be obtained through our RightsLink service via the Permissions link on the article page on our site—for further information please contact journals.permissions@oup.com.

older temporal constraints (Nesbitt and Ezcurra 2015, Martz and Parker 2017).

Globally, biostratigraphic models and detrital zircon ages constrain the oldest dinosaurs to the mid–late Carnian (*Hyperodapedon* Assemblage Zone) of the Candelária Sequence in Brazil (c. 233 Mya) (Langer *et al.* 2018, Schultz *et al.* 2020), lower Ischigualasto Formation, Argentina (c. 230 Mya) (Desojo *et al.* 2020), Pebbly Arkose Formation, Zimbabwe (Griffin *et al.* 2022), and the lower Maleri Formation (Langer *et al.* 2010, Kammerer *et al.* 2016), India. The lack of Carnian-aged Laurasian dinosaurs has been hypothesized to reflect inhospitable environmental barriers (Dunne *et al.* 2021, Kent and Clemmensen 2021, Griffin *et al.* 2022) that isolated high-latitude faunas until conditions improved during the Carnian Pluvial Episode (CPE), which is linked with a global increase in humidity lasting ~2 Myr (c. 234–232 Mya) (Simms and Ruffell 1989, Dal Corso *et al.* 2020, Simms and Drost 2024). Despite increased sampling and improved high-resolution radioisotopic dating techniques refining our understanding of the spatiotemporal distribution of the earliest dinosaurs and their kin (Irmis *et al.* 2011, Langer *et al.* 2018, Philipp *et al.* 2018, Desojo *et al.* 2020, Rasmussen *et al.* 2020, Lovelace *et al.* 2024), there continues to be an apparent dearth of northern hemisphere Carnian-aged dinosaur body-fossils.

As such, the diachronous rise hypothesis, which suggests dinosaur origins as a Gondwanan phenomenon (Irmis *et al.* 2011, Lee *et al.* 2018, Kent and Clemmensen 2021, Griffin *et al.* 2022), has largely relied on an absence of body-fossils in the northern hemisphere. Alternatively, the apparent absence of Carnian-aged dinosaurs in Laurasia can be explained by a paucity of well-studied time-equivalent terrestrial strata, most of which lack radioisotopic age control (Lovelace *et al.* 2024). Only a few Laurasian units have yielded faunal assemblages similar to those from chronostratigraphically similar Gondwanan strata (Fig. 1) (Benton and Walker 2010, Milroy *et al.* 2019, Zeh *et al.* 2021, Lovelace *et al.* 2024, Tourani *et al.* 2023, Simms and Drost 2024). The distribution of Carnian traces (e.g. UWGM 7435) across Laurasia attributed to dinosauromorphs (including dinosaurs) further support the sampling bias explanation. These traces demonstrate the presence of Dinosauria well before the first temporally constrained northern hemisphere dinosaur body-fossils (Bernardi *et al.* 2018). However, these data should not be over extrapolated beyond simply indicating the presence of this clade where traces are known.

Here we report the first dinosauromorphs, including a new sauropodomorph dinosaur and an indeterminate silesaurid along with high-resolution radioisotopic detrital ages from the Late Triassic (Carnian) Popo Agie Formation of Wyoming, USA. Although often fragmentary, the lower Popo Agie fossil assemblage (Fig. 1C) is known to include metoposaurids (Kufner *et al.* 2023), hyperodapedontine rhynchosaurs (Fitch *et al.* 2023), and loricatans (Dawley *et al.* 1979, Nesbitt *et al.* 2020b). Our findings of a novel species of sauropodomorph dinosaur from mid–late Carnian deposits in the northern hemisphere demonstrate the unambiguous presence of dinosaurs at low latitudes in strata chronostratigraphically equivalent to the oldest Gondwanan dinosaur faunas. Vertebrate remains are still considered to be relatively rare in the Popo Agie Formation (Lovelace *et al.* 2024),

with the notable exceptions being two mass death assemblages dominated by metoposaurid (Kufner and Lovelace 2018) and laticospid (So *et al.* 2024) stereospondyls. Although our study demonstrates the presence of at least one dinosaur (or more depending on future consensus on the phylogenetic position of ornithischians relative to silesaurids), the relative abundance of dinosaurs in the Popo Agie fauna is still equivocal. Regardless, these new data challenge the diachronous rise hypothesis and call into question the impermeability of Pangaeon latitudinal environmental barriers during the early-mid Carnian. This new assemblage is strongly reminiscent of those of dinosaur-bearing, high-latitude Gondwanan strata, making it unambiguously the oldest such assemblage in the northern hemisphere, and the oldest known low-latitude dinosaur globally.

METHODS

CA-ID-TIMS (Chemical Abrasion Isotope Dilution Thermal Ionisation Mass Spectrometry) U–Pb detrital zircon analyses
Zircon crystals selected on the basis of previous previously published LA-ICP-MS (Laser Ablation Inductively Coupled Mass Spectrometry) spot analysis (Lovelace *et al.* 2024) were removed from the epoxy mounts and subjected to a modified version of the chemical abrasion method (Mattinson 2005), whereby single crystals were partially dissolved in a single step with concentrated hydrofluoric acid at 190°C for 12 h. After rinsing and ultrasonication, residual crystals were spiked with the ET535 mixed tracer solution (Condon *et al.* 2015), fully dissolved in concentrated hydrofluoric acid at 220°C for 48 h, dried, and re-dissolved in 6M hydrochloric acid at 180°C for 12 h. U and Pb were purified by anion exchange chromatography (Krogh 1973), eluted together, and loaded on a single zone-refined rhenium filament with a mixed silica gel and dilute phosphoric acid solution for mass spectrometry (Gerstenberger and Haase 1997). U–Pb geochronology methods for isotope dilution thermal ionization mass spectrometry (ID-TIMS) following (Macdonald *et al.* 2018).

Pb and U isotope ratios were measured on an IsotopX Isoprobe-T thermal ionization mass spectrometer by single collector peak jumping on a Daly conversion dynode ion-counting detector (Pb⁺) or static multicollection on Faraday cups fitted with 10¹² W resistor amplifiers (UO₂⁺). U–Pb dates and uncertainties for each analysis were calculated using the algorithms of (Schmitz and Schoene 2007), the U decay constants of Jaffey *et al.* (Jaffey *et al.* 1971), and the ²³⁸U/²³⁵U ratio of Hiess *et al.* (Hiess *et al.* 2012). Propagated uncertainties are based upon non-systematic analytical errors, including counting statistics, instrumental fractionation, tracer subtraction, and blank subtraction. All CA-ID-TIMS data are reported in the Supporting Information, Table S1.

Age-modelling

An age model was generated using the R package ‘modifiedBChron’ to estimate the upper and lower boundaries of the Upper Triassic Popo Agie Formation. The basis of the model is ‘BChron’, a Bayesian age-depth model implemented in R (Haslett and Parnell 2008). BChron was originally built to include radiocarbon analyses; however, it lacked necessary features

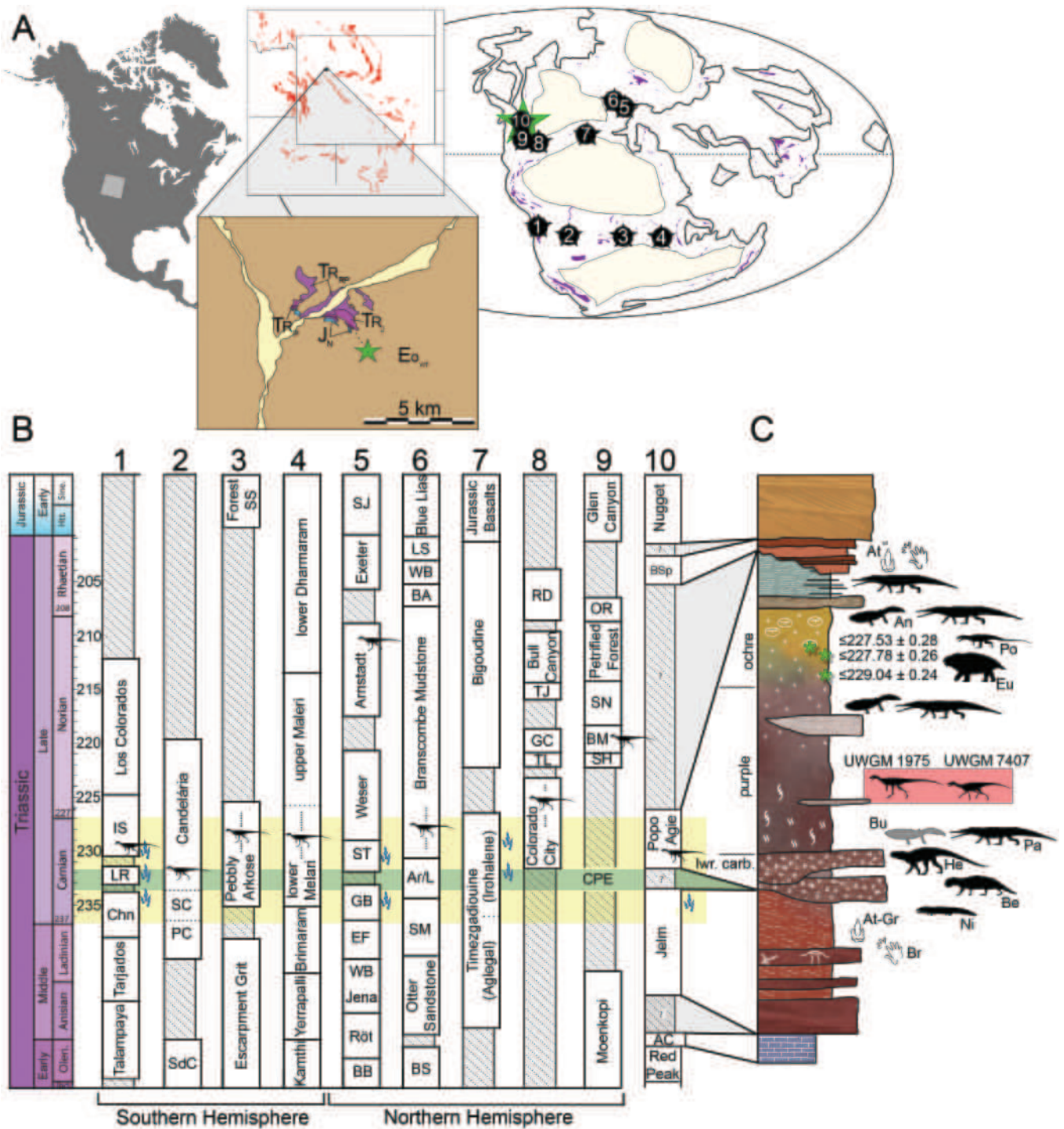


Figure 1. A palaeogeographic map (A) of Triassic outcrops shows the position of key localities (1 to 9); Chugwater Group, Wyoming, USA (inset), local geology surrounding Garrett's Surprise (star). Chronostratigraphic context of early dinosaur-bearing units (B) shows the relative stratigraphic positions for first occurrences of dinosaurian body and trace fossils tied to a generalized stratigraphic section (C) of the upper Chugwater Group [after Lovelace *et al.* (2024)]. The shaded box highlights the stratigraphic position of UWGM 1975 and UWGM 7407 within the Popo Agie Formation. Localities: 1, Argentina; 2, Brazil; 3, Zimbabwe; 4, India; 5, Germany; 6, Britain; 7, Morocco; 8, Texas, USA (Dockum Group); 9, south-western USA (Chinle/Moenkopi formations); 10, Wyoming, USA (Chugwater Group). Silhouettes (not to scale) on outcrop demonstrate faunal distribution within the Popo Agie and Jelmin formations. At, *Atreipus* sp.; At-Gr, *Atreipus-Grallator* plexus; An, *Anaschisma browni*; Be, *Beesiiwo coowuse*; Bu, *Buettnererpeton bakeri*; Br, *Brachychirotherium* sp.; Eu, *Eubrachiosaurus browni*; He, *Heptasuchus clarki*; Pa, *Parasuchus bransonii*; Po, *Poposaurus gracilis*; Ni, *Ninumbehan dookoodukah*. Artist credits for silhouettes from Phylopic.org and abbreviated formation names provided in the Supporting Information, Text S1. Previously published dinosaur-bearing localities recovered from PBDB (PaleobioDB.org; accessed Feb, 2024; Supporting Information, Data S1).

for deep time modelling. The Bchron code was modified (Trayler *et al.* 2020) to incorporate individual dates that can be grouped into a single age distribution as is common in U–Pb geochronology (i.e. ‘modifiedBchron’). Three CA-ID-TIMS maximum depositional age distributions were used to constrain the upper and lower bounds of the ochre unit within the upper Popo Agie Formation (Lovelace *et al.* 2024; Supporting Information, Text S1 (Age-depth modeling)).

Histological sampling

Prior to sectioning, the femur UWGM 7549 was measured, 3D scanned, and photographed to document original morphology. A 1-cm thick block was extracted from just distal to the femoral head, at the most proximal end of the diaphysis, using a high-speed diamond saw. The 1-cm wafer was then prepared using traditional hard-tissue histology sampling techniques (Padian and Lamm 2013). We studied the bone microstructure with a petrographic microscope (Nikon Eclipse 50iPOL) in plane-polarized (PPL) and cross-polarized (XPL) light. We employed XPL light with a lambda compensator to distinguish between areas of anisotropic and isotropic bone mineral organization. Photomicrographs were taken with this microscope and a Nikon DS-Fi1 digital camera, and composite images for our thin-sections were compiled with NIS-Elements BR 4.20 (see below). We employ the osteohistological terminology of Francillon-Vieillot *et al.* (Francillon-Vieillot *et al.* 1990) and Buffrénil *et al.* (de Buffrénil *et al.* 2021). All thin sections are curated in the University of Wisconsin Geology Museum (UWGM). Additional copies of thin-sections are housed at Macalester College in St. Paul, Minnesota, United States. High-resolution photomicrographs are also archived in Morphosource.org ID: 000607948.

Phylogenetic analyses

To assess the phylogenetic position of UWGM 1975, UWGM 7549, and UWGM 7407, we tested the matrix of Garcia *et al.* (2023; Supporting Information, Text S2) based on the matrix of Norman *et al.* (2022) with maximum parsimony using TNT v.1.5 (Goloboff and Catalano 2016) and Bayesian inference using MrBayes v.3.2.6 (Huelsenbeck and Ronquist 2001, Ronquist and Huelsenbeck 2003). This matrix captures a broad taxonomic sample of avemetatarsalians with an extensive sampling of Triassic dinosauromorphs. We added six characters from previous studies (Ezcurra and Brusatte 2011, Ezcurra 2017, Pol *et al.* 2021) and six novel characters to encompass known variation in the astragalus of early Dinosauroomorpha. We modified 12 characters from the original matrix (Garcia *et al.* 2023) and one added character (Ezcurra 2017) in order to improve clarity in phrasing, to improve consistency with previous work, or to capture variation in astragalus anatomy that was either unrecognized prior to this study or revealed from UWGM 1975 (see full details in the Supporting Information, Text S2 character list). We reassessed character-state scores for the pre-existing matrix using the primary literature or direct observation and made changes where necessary. We analysed two versions of this matrix to ensure that UWGM 7549 could be reliably referred to the same taxon as the astragalus UWGM 1975 and to test the phylogenetic position of UWGM 1975 and UWGM 7549 with all evidence: one with a combined OTU of both the astragalus and the referred femur

(combined OTU matrix; Supporting Information, Data S2, S3) and one with separate operational taxonomic units (OTUs) for the holotype astragalus and the referred femur (split OTU matrix; Supporting Information, Data S4, S5). In addition, the proximal end of a silesaurid femur UWGM 7407 and the distal end of a humerus UWGM 7550 from Garrett’s Surprise were combined into a single OTU. Characters 4, 13, 25, 82, 84, 87, 89, 109, 142, 150, 166, 174, 175, 184, 186, 190, 201, 203, 205, 208, 209, 211, 212, 225, 234, 235, 236, 239, 250, 252, 255, 256, and 275 were treated as additive, following Garcia *et al.* (2023). *Euparkeria capensis* Broom, 1913 was designated as the primary outgroup in all analyses.

Maximum parsimony analysis was performed in TNT v.1.5 (Goloboff and Catalano 2016) following the methods outlined by Hartman *et al.* (2019). An initial driven search was conducted using the New Technology search option (sectorial search, drift, ratchet, and tree fusing enabled) for both the combined OTU matrix and the split OTU matrix. After the initial New Technology search, trees from RAM were re-analysed using the New Technology search with ‘CSS’ in ‘Sect. Search’ disabled for a minimum of 10 iterations once no change in the number of MPTs was observed, and a strict consensus of these MPTs was calculated. Bremer support decay indices were calculated in TNT using the ‘BREMER.RUN’ script. Strict consensus trees were resampled using jackknifing and standard bootstrapping with replacement using 1000 pseudoreplicates and default parameters in TNT v.1.5.

Bayesian phylogenetic inference was performed with MrBayes v.3.2.6 (Huelsenbeck and Ronquist 2001, Ronquist and Huelsenbeck 2003) using the combined OTU matrix and the split OTU matrix with a gamma distribution of rates allowing for some invariable character states (‘invgamma’). Two simultaneous runs of four chains were allowed to run for 30 000 000 iterations and 25% of trees were discarded as burn-in. After 30 000 000 iterations, the runs converged to result in an average standard deviation of split frequencies stably below 0.01. Nodes with <0.5 posterior probability (PP) were considered poorly supported, and two consensus trees for each matrix were generated: one with complete bifurcation (tree computed using ‘contype = allcompat’) and one with nodes <0.5 PP collapsed (‘contype = halfcompat’).

μCT scans

UWGM 1975, 7549, 7550, 7407, and 7434 were scanned on a Phoenix v|tome|x s 240 with a dual 180 tube at the University of Chicago’s Department of Organismal Biology and Anatomy PaleoCT lab (RRID:SCR_024763). Different anatomical elements were scanned with slightly different settings. As such, data sheets for each scan’s specific parameters are included with each image dataset archived in Morphosource.org [ID:000607552 (femur); 000607470 (astragalus)]. All μCT data was segmented and analysed in the ORS software DRAGONFLY under a free annual academic licence. Meshes made in dragonfly were exported as .stl or .obj for import into the open source 3D software BLENDER where models were visualized.

Nomenclatural statement

Western taxonomy has a history deeply rooted in colonialism (Browne 1992, Schiebinger 2004, Endersby 2010, Liboiron

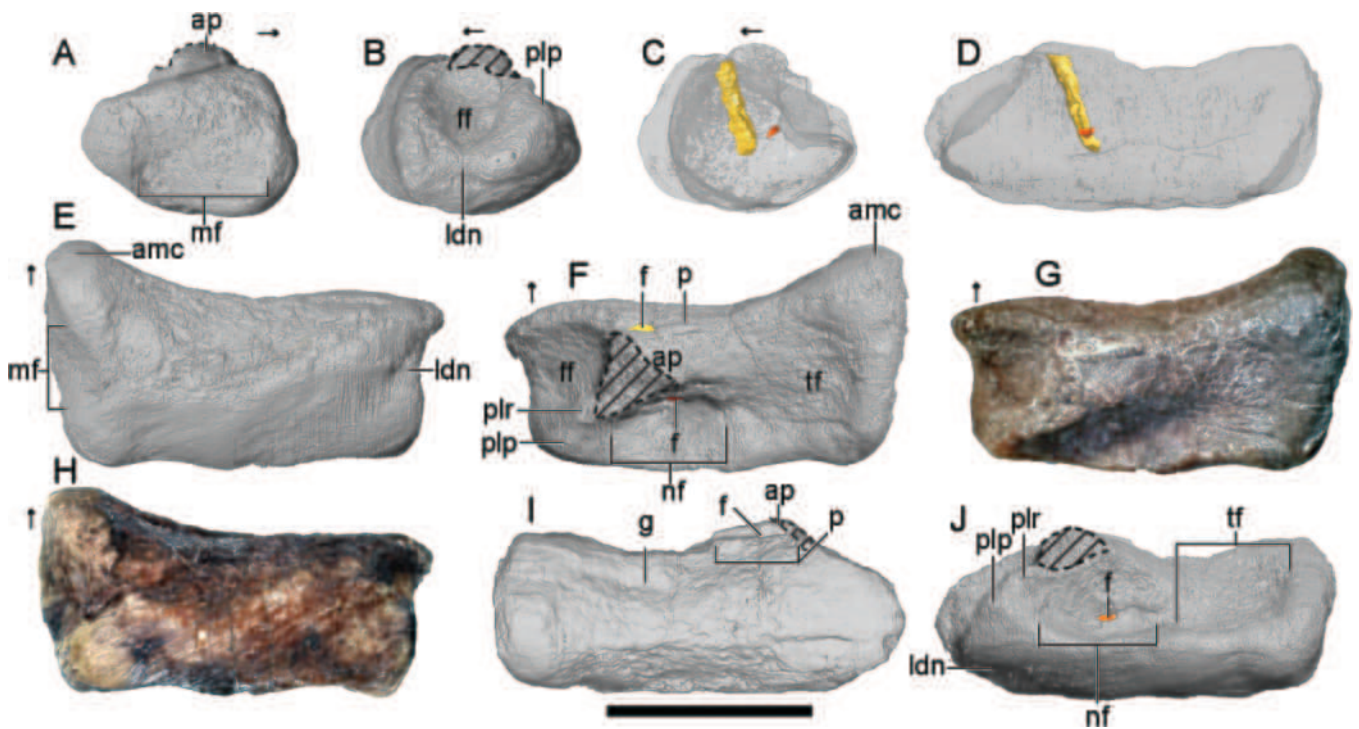


Figure 2. Holotype left astragalus of *Ahvaytum bahndooiveche* gen. et sp. nov. (UWGM 1975). 3D model in (A) medial, (B) lateral, (C) lateral transparent, (D) posterior transparent, (E) distal, (F) proximal, (I) anterior, and (J) posterior orthographic views. Photographs in (G) proximal and (H) distal views. Abbreviations: amc, anteromedial corner; ap, ascending process of the astragalus; g, groove; f, foramen; ff, fibular facet; ldn, laterodistal notch (= lateroventral depression); mf, medial fossa; nf, non-articular fossa (= dorsal basin, = semi-elliptical fossa); p, platform; plp, posterolateral process; plr, posterolateral ridge; tf, tibial facet. Diagonal lines indicate broken surfaces. Arrows indicate anterior direction. Scale bar = 1 cm. STL models archived online (morphosource.org ID: 000607569).

2021, Monarrez *et al.* 2022) that is unknown, unrecognized, or unacknowledged by many practitioners. Taxa are often given names that reflect geographic features, regions, or waterways named by colonizers who did not recognize or validate pre-existing Indigenous names (Gillman and Wright 2020). In recent years there has been a push to make the sciences more inclusive and to promote representation by highlighting regional, linguistic, and cultural diversity in communities within which research is being conducted around the world (Wilder *et al.* 2016, Rummy and Rummy 2021). There have been calls for nomenclatural changes that range from promoting a more inclusive approach to erecting new taxa (Rummy and Rummy 2021, Orr *et al.* 2023), to larger more regulated systemic changes, including the discontinuance of eponyms (Gillman and Wright 2020, Cheng *et al.* 2023, Guedes *et al.* 2023), and counterpoints to these arguments (Palma and Heath 2021, Pethiyagoda 2023). In many cases visiting researchers and local communities can benefit through long-term partnerships (Wilder *et al.* 2016), including the naming of new taxa in local languages with local input (Shubin *et al.* 2006, Rummy and Rummy 2021, Jost *et al.* 2023, Orr *et al.* 2023). The publication of this name, created by Eastern Shoshone students and Elders, is intended to honour the Eastern Shoshone people, their language, and the land to which they belong.

Data availability

Derived μ CT scan data, resulting post segmentation 3D (.stl) models, light scans, and histology data are made publicly available through Morphosource.org; dataset IDs are listed in text.

Systematic palaeontology

Dinosauromorpha Benton, 1985 (*sensu* Nesbitt 2011)

Dinosauriformes Novas, 1992 (*sensu* Nesbitt 2011)

Dinosauria Owen, 1842 (*sensu* Padian and May 1993)

Saurischia Seeley, 1887 (*sensu* Gauthier 1986)

Sauropodomorpha(?) von Huene, 1932

Ahvaytum gen. nov.

Etymology: *Ahvaytum*, from the Shoshone 'Aⁿva-tum' (pronounced 'ah-vay-tum'), meaning 'long ago' in reference to the ancient nature of UWGM 1975. Pronunciation guide: the sound ah is as in 'autumn', vay as in 'vague', and tum as in 'autumn'. See Supporting Information, Audio S1 (discussion of name); recordings by Eastern Shoshone Elder (RT).

Type species: *Ahvaytum bahndooiveche*.

Diagnosis: As for type species, by monotypy.

Ahvaytum bahndooiveche sp. nov.

(Fig. 2).

Holotype: UWGM 1975, isolated left astragalus (Fig. 2).

Referred material: The proximal end of a left femur (UWGM 7549; Fig. 3) is referred to *Ahvaytum bahndooiveche* due to clear saurischian affinities. This femur was found *ex situ* within a 5-m radius of the type specimen and encrusted with a similar micritic carbonate.

Etymology: *bahndooiveche*, from the Shoshone ‘ban-döi-ve-che’ (pronounced ‘bon-do-ee-vee-chee’), meaning ‘water’s young

handsome man’ in reference to the colourful salamanders found in the region, and also means ‘dinosaur’ (Supporting Information, Audio S1), which is the meaning used here. The name *Ahvaytum bahndooiveche* (‘long ago dinosaur’) is the product of a multigenerational collaboration between the Fort Washakie Schools 7th grade cohort (2022), educators, Eastern Shoshone Tribal Historic Preservation Office, and Tribal Elders. Pronunciation guide: bahn as in ‘bonnet’,

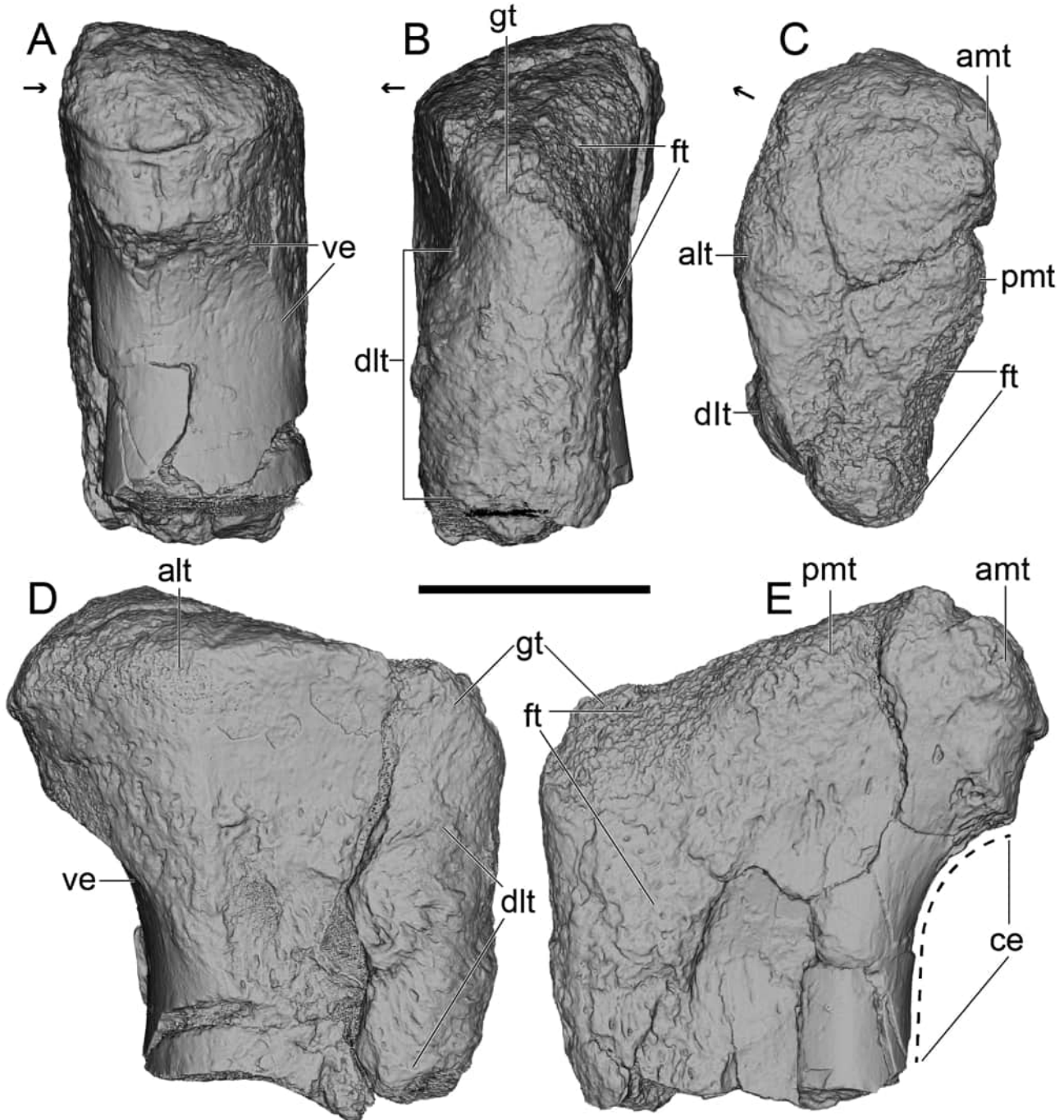


Figure 3. Proximal end of a left femur UWGM 7549 (A–E) referred to *Ahvaytum bahndooiveche* gen. et sp. nov.). 3D model in (A) anteromedial, (B) posterolateral, (C) proximal, (D) anterolateral, and (E) posteromedial orthographic views. Abbreviations: alt, anterolateral tuber; amt, anteromedial tuber; ce, concave emargination; dlt, dorsolateral trochanter; ft, fossa trochanterica (= facies articularis antitrochanterica); gt, ‘greater trochanter’; pmt, posteromedial tuber; ve, ventral emargination. Arrows indicate anterior direction. Scale bar = 1 cm. STL models archived online (morphosource.org ID: 000607572).

do-ee as in ‘dewy’, vee as in ‘ivy’, and chee as in ‘cheese’. See the [Supporting Information, Audio S1](#) for recorded pronunciation (recording by RT. LSID urn:lsid:zoobank.org:pub:538C156C-5CC1-4706-8D8A-FFA6757A6590).

Locality and horizon: Garrett’s Surprise (after undergraduate field assistant Garrett Johnson who discovered the locality) is a small exposure of the Popo Agie Formation found in an erosional window within the overlying Wind River Formation (Eocene), on Wyoming Game and Fish administered lands, c. 1 km south of the confluence of the East Fork of the Wind River and Spear Creek ([Fig. 1A](#)). GPS coordinates for Garrett’s Surprise are repositied with the type specimen. Vertebrate material was surface collected and no *in situ* specimens were recovered during a screening effort of the area; all material is constrained to the mid to upper part of the purple unit of the lower Popo Agie Formation ([Lovelace et al. 2024](#)). The ochre unit is poorly exposed along the fall line where specimens were collected and is unconformably overlain by Eocene deposits of the Wind River Formation [see [Supporting Information, Text S1](#) (Fieldwork and Site Details)].

Diagnosis: *Ahvaytum bahndooiveche* shares a combination of features present in sauropodomorph dinosaurs to the exclusion of theropods, herrerasaurs, and ornithischians, including: a flat, roller-shaped distal surface of the astragalus shared with sauropodomorphs but not herrerasaurs and neotheropods ([Marsh et al. 2019](#)); a tibial facet that does not extend on to the anteromedial corner of the astragalus shared with all sauropodomorphs in our study, the silesaurid *Lewisuchus admixtus* [Romer, 1972](#), the theropods *Lepidus praecisio* and *Eodromaesus murphi* [Martinez et al., 2011](#), and the herrerasaurs *Tawa hallae* [Nesbitt et al., 2009](#) and *Chindesaurus bryansmalli* [Long and Murry, 1995](#); a shallow laterodistal notch of the astragalus shared with non-massopodan sauropodomorphs, except *Panphagia protos* [Martinez and Alcober, 2009](#) and *Efraasia minor* [von Huene, 1875 \(sensu Galton 1973\)](#) and the herrerasaur *T. hallae*; a rounded anterior and medial margin on the proximomedial surface of the astragalus shared with the theropod *Eodromaesus murphi* and sauropodomorphs, except *Saturnalia tupiniquim* [Langer et al., 1999](#) and a referred specimen of *Buriolestes schultzi* [Cabreira et al., 2016 \(sensu Moro et al. 2024\)](#); a posterolateral ridge between the anterior ascending process and the posterolateral process that is always taller than the posterolateral process shared with the herrerasaurids *Herrerasaurus ischigualastensis* [Reig, 1963](#) and *Sanjuansaurus gordilloi* [Alcober and Martínez, 2010](#) and sauropodomorphs, except *Unaysaurus toletinoi* [Leal et al., 2004](#). *Ahvaytum bahndooiveche* is differentiated from all other sauropodomorphs with comparable material by the following autapomorphy: fossa on the medial surface of the astragalus that is open distally. *Ahvaytum bahndooiveche* is differentiated from *Eoraptor lunensis* [Sereno et al., 1993](#), *Mbiresaurus raathi* [Griffin et al., 2022](#), *P. protos*, *S. tupiniquim*, and a referred specimen of *B. schultzi* by a proportionally wider astragalus (max. anteroposterior length/max. transverse width: *Ahvaytum* = 0.53, *Buriolestes* \cong 0.71, *Eoraptor* \cong 0.63, *Mbiresaurus* \cong 0.64, *Panphagia* \cong 0.88, and *Saturnalia* \cong 0.73) and by a relatively wide fibular facet occupying more than a quarter of the transverse width of the astragalus. Further differentiated from *Eoraptor lunensis* by a posteromedial

angle on the astragalus. Further differentiated from a referred specimen of *B. schultzi* ([Moro et al., 2024](#)) by a poorly proximally expanded posteromedial process (= pyramidal process of some authors) and by a relatively tall posterolateral process (= posterior ascending process of some authors). Further differentiated from both *B. schultzi* and *M. raathi* by a posterolateral process that is level with the posterior margin of the astragalus in proximal view.

Remarks: The proximal end of a silesaurid femur (UWGM 7407) and the distal end of a probable silesaurid humerus (UWGM 7550; see below) were recovered from the study area precluding the referral of 15 non-diagnostic dinosauro-morph elements (UWGM 7434; [Supporting Information, Fig. S1 in Text S1](#)) to higher taxa. Additional vertebrate material was surface collected from the Garrett’s Surprise locality and identified as non-ornithodiran or indeterminate.

Description: The type specimen of *Ahvaytum bahndooiveche* (UWGM 1975) is an isolated left astragalus ([Fig. 2](#)). A calcaneum was not recovered and there is no evidence of fusion of these elements. The transverse width of the astragalus is nearly twice its maximum anteroposterior length. The proximal surface is slightly weathered, but the rest of the surface of the element is essentially intact. There is a transverse groove on the anterior surface of the body of the astragalus, which is widespread among dinosauro-morphs. The ascending process is separated from the anterior surface by a platform and broken at approximately mid-height. A foramen on the anterior surface of the ascending process extends posterodistally into the body of the astragalus. A posterolateral ridge extends from the ascending process to meet a posterolateral process [= posterior ascending process of [Sereno and Arcucci \(1994\)](#)] along the posterior margin. The anteromedial corner is acute as in other early dinosaurs (e.g. [Müller 2021](#)) and projects well beyond the anterolateral condyle. The tibial articular facet is separated from the anterior and medial margins by a wide, rounded lip and does not extend on to the anteromedial corner, which is identical to the condition in several sauropodomorphs (e.g. [Müller 2021](#)). The medial surface of the astragalus bears a fossa that opens toward the distal surface, which appears to be autapomorphic among dinosaurs. The posteromedial margin forms a corner, and the proximal margin here is not raised into a pyramidal process such as that found in theropods (e.g. [Nesbitt and Ezcurra 2015](#)) or the elevated crest in unaysaurids (e.g. [Müller 2021, Ezcurra et al. 2023](#)). Posterior to the ascending process there is a non-articular fossa (= dorsal basin, = semi-elliptical fossa) with a weathered but raised rim along its medial margin. Within this fossa there is a single oblong vascular foramen whose canal is short and anteriorly directed at the base of the ascending process ([Figs. 2C–D](#)). The fibular facet occupies just over a quarter of the transverse width of the astragalus and is delineated by a sharp medial margin. A laterodistal notch (= lateroventral depression) is present on the distal surface, presumably for reception of a medial process of the calcaneum, as is the case in *Eoraptor lunensis* ([Sereno et al., 2012](#)). An incipient protuberance is present on the distolateral surface of the astragalus just anterior to the laterodistal notch; however, unlike the condition in the unaysaurids *Jaklapallisaurus asymmetricus* [Novas et al., 2010](#) and *Macrocollum itaquii* [Müller](#)

et al., 2018 (Ezcurra *et al.* 2023: fig. 3e–g) it does not form a distinct projection.

Referred material: The proximal end of a left femur (UWGM 7549) possesses several dinosaurian and saurischian features but is too incomplete for a referral beyond Saurischia on its own (Fig. 3). The proximal surface of the femur appears to be slightly abraded revealing trabecular bone and hindering the identification of a transverse groove, such as that seen in UWGM 7407 (Fig. 4F) and widespread among early-diverging sauropodomorphs and dinosauromorphs more generally. There are also several cracks present in this element, one of which passes through the position that would be occupied by

a ligament sulcus between the anteromedial and posteromedial tubera. The posteromedial tuber is small and rounded, and the larger anteromedial tuber is also rounded. The anterolateral tuber forms a broad, rounded profile along the anterolateral surface of the femur in proximal view. The head of the femur is offset from the shaft resulting in a concave emargination just ventral to the head, common among all dinosaurs. On the anterolateral surface of the femur, a ridge extends from the ventral margin of the head then merges distally into the shaft forming a ventral emargination, such as that seen in *Saturnalia tupiniquim*, *Nhandumirim waldsangae* Marsola *et al.*, 2018, and some coelophysoids (Kirmse *et al.* 2023), but unknown among core ornithischians, exclusive of silesaurids. The shaft of the femur

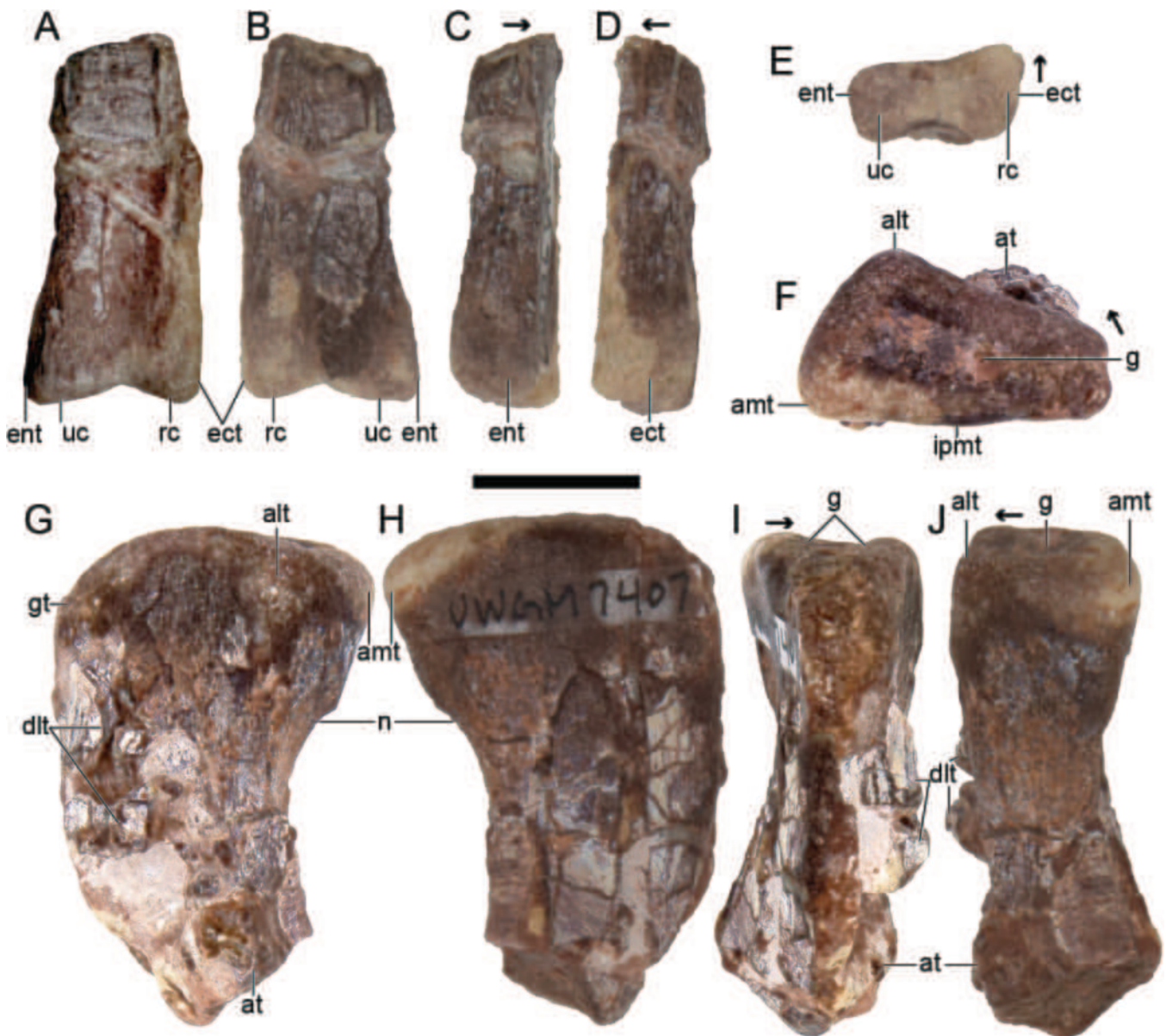


Figure 4. Photographs of sulcimentisaurian silesaurid elements from the Garrett's Surprise locality. Distal end of a left humerus UWGM 7550 (A–E) in (A) anterior, (B) posterior, (C) medial, (D) lateral, (E) and distal views. Proximal end of a right femur UWGM 7407 (F–J) in (F) proximal, (G) anterolateral, (H) posteromedial, (I) posterolateral, and (J) anteromedial views. Abbreviations: alt, anterolateral tuber; amt, anteromedial tuber; at, anterior trochanter; dlt, dorsolateral trochanter; ect, ectepicondyle; ent, entepicondyle; g, groove; gt, greater trochanter; ipmt, incipient posteromedial tuber; n, notch; rc, radial condyle; uc, ulnar condyle. Arrows point in the anterior direction. Scale bar equals 1 cm.

is broken approximately just above the position of the anterior trochanter. The dorsolateral trochanter is present as a rounded rugosity along the lateral side of the femoral shaft and probably missing its distal extent due to the break. The 'greater trochanter' is prominent and squared off with a straight margin between it and the head of the femur in anterior/posterior view similar to *Herrerasaurus ischigualastensis* (Novas, 1994) and some specimens of *Pampadromaeus barberenai* (Cabreira *et al.*, 2011) and *Buriolestes schultzi* (Müller, 2022). The fossa trochanterica (= facies articularis antitrochanterica) along the posterior side of the 'greater trochanter' is ventrally (= distally) descended, which is common among dinosaurs (Nesbitt, 2011).

Ontogenetic assessment: Both the holotype astragalus (UWGM 1975) and referred femur (UWGM 7549) exhibit smooth bone textures and prominent condyles that are consistent with relatively older ontogenetic status in this specimen (Griffin *et al.* 2019). Similarly, the referred femur exhibits muscle scars that are robustly developed and also support the notion of an older ontogenetic status for UWGM 7549. An external fundamental system (EFS) is absent from the femoral cross-section (see below); its presence would indicate the attainment of skeletal maturity. That said, other osteohistological signatures are consistent with a more advanced ontogenetic status for UWGM 7549. These data include the presence of endosteal remodelling around the medullary cavity forming an internal fundamental system (IFS), cortical remodelling that extends into the mid-cortex alongside a transition to more highly organized and less vascularized primary bone tissue at the periosteal margin, which signals a decrease in primary bone apposition in later ontogeny. A lack of an EFS indicates that UWGM 7549 was still slowly growing at the time of death. In light of these histological details, the absence of lines of arrested growth (LAG) in UWGM 7549 should not be presumed to indicate an individual less than a single year of age. Instead, this individual had probably progressed beyond earliest ontogeny.

Dinosauromorpha Benton, 1985 (*sensu* Nesbitt 2011)

Dinosauriformes Novas, 1992 (*sensu* Nesbitt 2011)

Silesauridae Langer *et al.*, 2010

Sulcimentisauria Martz and Small, 2019

Sulcimentisauria gen. et sp. indet.

(Fig. 4)

Referred material: UWGM 7550, the distal end of a left humerus and the proximal end of a right femur, UWGM 7407.

Locality and horizon: The Garrett's Surprise locality from the purple unit of the Popo Agie Formation (see further details above).

Remarks: The silesaurid affinities of UWGM 7407 are readily determined by the following combination of features: a notch ventral to the anteromedial tuber; a subtriangular proximal outline due to a prominent anterolateral tuber and incipient posteromedial tuber; and a transverse groove on the proximal

surface of the femur (Martz and Small 2019). The silesaurid affinities of the distal humerus UWGM 7550 are less certain, but it compares favourably with the morphology of the Moroccan silesaurid *Diodorus scytobrachion* Kammerer *et al.*, 2012. We will refer to the combined OTU of UWGM 7407 and UWGM 7550 simply as UWGM 7407, unless specifically referring to the femur or humerus, then the element will be included and the catalogue number in parentheses. The combined character states found in the femur (UWGM 7407) are also present in *Di. scytobrachion*, *Sacisaurus agudoensis* Ferigolo and Langer, 2007, and *Silesaurus opolensis* Dzik, 2003; unfortunately the characters that differentiate these taxa are damaged, obscured, or entirely missing in UWGM 7407 (Fig. 4).

Description: The humerus (UWGM 7550) is fragmentary with only the distal end preserved and significant fracturing through the shaft. The anatomical orientation of the distal end of this silesaurid humerus is complicated by the presence of torsion in the humerus of *Kwanasaurus williamparkeri* Martz and Small, 2019 and lack thereof in other sulcimentisaurian silesaurids (Dzik 2003, Kammerer *et al.* 2012) and the non-sulcimentisaurian silesaurid *Asilisaurus kongwe* Nesbitt *et al.*, 2010, so all interpretations of orientation assume no humeral torsion as is plesiomorphic for silesaurids. The only character relevant to the character matrix determined from the humerus is that the distal condyles are relatively narrow relative to the humeral shaft, as is typical for sulcimentisaurian silesaurids (e.g. Dzik 2003, Kammerer *et al.* 2012), in contrast to the broader distal humerus of non-sulcimentisaurian silesaurids (Ezcurra *et al.* 2020b, Nesbitt *et al.* 2020a). The radial and ulnar condyles both form rounded, subtriangular projections with a notch between them, as opposed to the more well-developed condyles of non-sulcimentisaurian silesaurids (Ezcurra *et al.* 2020b, Nesbitt *et al.* 2020a). The ulnar condyle is slightly larger than the radial condyle and has a medial margin that is more posteriorly projected. On both the anterior and posterior face of the humerus above the condyles, there is a fossa that extends about 1 cm on to the humeral shaft.

The proximal outline of the femur (UWGM 7407) is subtriangular due to the presence of a prominent anterolateral and anteromedial tuber and significant reduction of the posteromedial tuber and straight margins between these features. A straight, transverse groove is present along the proximal surface. A notch is present distal to the head of the femur, which is ubiquitous among silesaurids (e.g. Martz and Small 2019). The dorsolateral trochanter is broken and displaced across the anterolateral face, but what is preserved is ridge-like. The broken dorsolateral trochanter and surrounding matrix obscure a clear view of the anterior trochanter (= 'lesser trochanter'), but what is visible is mound-like. However, it cannot be determined if the anterior trochanter was small and confluent with the femoral shaft, as in non-sulcimentisaurian silesaurids, or if it was large and offset from the shaft by a cleft, as in sulcimentisaurians, some early core ornithischians, and some neotheropods. The 'greater trochanter' is prominent and rounded, and the fossa trochanterica (= facies articularis antitrochanterica) is level with the 'greater trochanter'. The femoral shaft curves slightly posteriorly, and the femur is broken above the fourth trochanter.

Plexus *Atreipus–Grallator*Ichnogenus *Atreipus* Olsen and Baird, 1986Ichnogenus *Grallator* Hitchcock, 1858

Referred specimens: UWGM 7435, a partial right pes trace preserved in concave epirelief was collected in the upper Jelm Formation along the Red Wall, Natrona County, Wyoming; UWGM 'Jelm Dino Track' site (Fig. 5).

Description: UWGM 7435 is a small (9.0×5.6 cm) partial pes impression preserving digits II–IV and, potentially, a very faint manus impression. The isolated slab was found *ex situ*, though confidently constrained to 1–2 m of stratigraphic thickness (topographic constraint) ~15 m below the top of the Jelm Formation. The track is located on a 21.5×12 -cm slab of fluvial sandstone with broad-wavelength, ripple-marked bedding; the preserved trace is digitigrade and tridactyl, mesaxononic where digit III is longest and potentially quadrupedal (Fig. 5). The pes digits are relatively straight, long, and slender with small acuminate claw impressions. Pads are observable, but not sharply defined. Digit IV is closely aligned to III with a 7.5° divarication. Digit III to II has just over double the divarication (17°). The impression of digit IV is *c.* 8 mm wide with little variance, while digits III and II are *c.* 13 and 11 mm, respectively. Although lacking morphological details, a faint impression anterolateral to pes digits II–III is interpreted to be a manus with three anterolaterally projected digits. Because of this ambiguity in manus identification, we consider this trace within the *Atreipus–Grallator* plexus, but cannot confidently assign it to either *Atreipus* or *Grallator*. Considering

the ecological implications of a *Grallator* (i.e. dinosaurian) tracemaker, we conservatively assign this trace to *Atreipus*.

RESULTS

Geochronology and age modelling

Youngest zircon crystals from three of five samples collected from three stratigraphic units of the upper Popo Agie Formation at two localities, previously analysed by LA-ICP-MS (Lovelace *et al.* 2024), were analysed using chemical abrasion ID-TIMS (Fig. 6A–C; Supporting Information, Table S1). Three crystals from the stratigraphically lowest sample (DH2) from an analcime-rich hydromorphic gleyed palaeosol near the Days Hill locality resulted in $^{206}\text{Pb}/^{238}\text{U}$ dates from 229.45 ± 0.16 to 229.03 ± 0.17 Mya. The youngest two grains yield a peak in the probability density plot corresponding to a maximum depositional age of $\leq 229.04 \pm 0.24$ Mya (2σ). Five crystals from the mid-upper analcime-rich ochre unit (DH1) resulted in $^{206}\text{Pb}/^{238}\text{U}$ dates from 228.71 ± 0.53 to 227.73 ± 0.20 Mya. The youngest three grains yield a peak in the probability density plot corresponding to a maximum depositional age of $\leq 227.78 \pm 0.26$ Mya (2σ). Four crystals were selected from the ROY sample collected from a stratigraphically limited exposure of the ochre unit about 8 km to the north of Days Hill and resulted in $^{206}\text{Pb}/^{238}\text{U}$ dates from 229.26 ± 0.26 to 227.34 ± 0.45 Mya. The youngest two grains yield a peak in the probability density plot corresponding to a maximum depositional age of $\leq 227.53 \pm 0.28$ Mya (2σ).

These results support a maximum depositional age for the base of the upper Popo Agie Formation of *c.* ≤ 229 Mya. The other two samples both support a maximum depositional age of no older than *c.* ≤ 228 Mya. While this provides the first

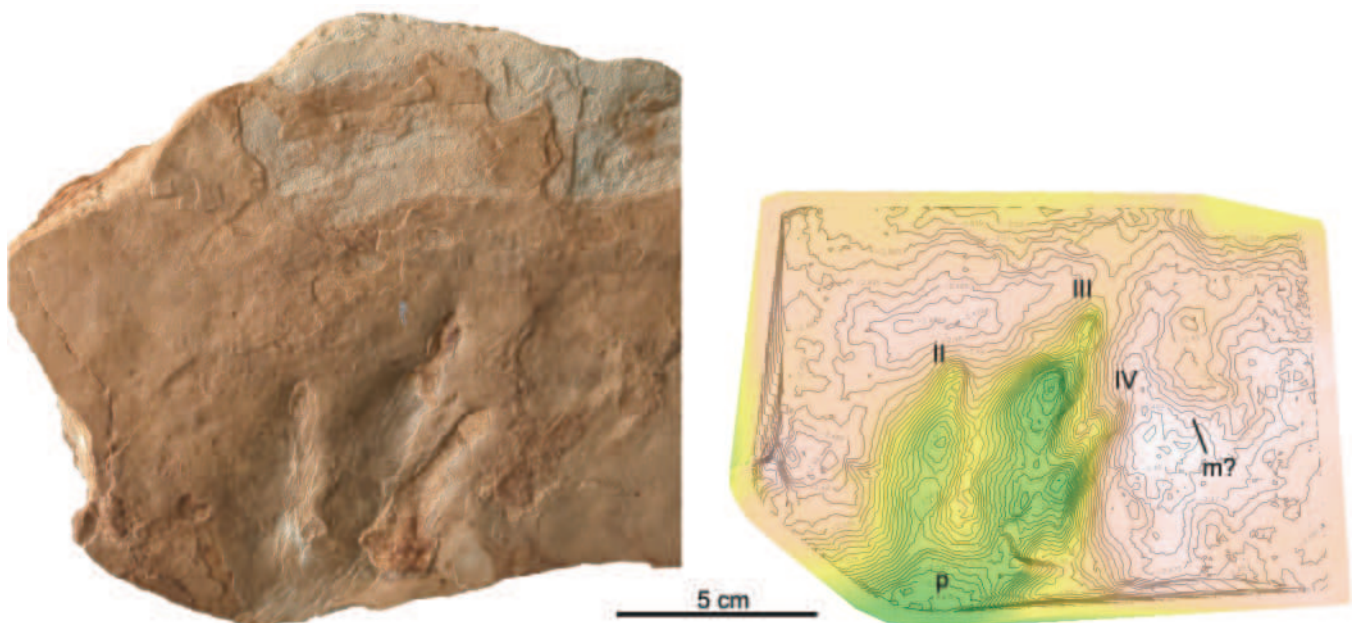


Figure 5. UWGM 7435 (left) is an isolated slab containing a single tridactyl pes and possible manus impression attributed to an *Atreipus–Grallator* plexus tracemaker from the upper Jelm Formation, Natrona County, WY, USA. A digital surface-depth map (right) produced in METASHAPE (v.2.0.3; Agisoft) from surface light-scans demonstrates the depth and toe pad delineations of pes (p) digits II–IV. The manus impression may be present (m?); other than a very slight depression there are no morphological features to confidently identify it as such. Scale bar is in 1-cm increments. Data reposted on Morphosource.org, ID: 000607578.

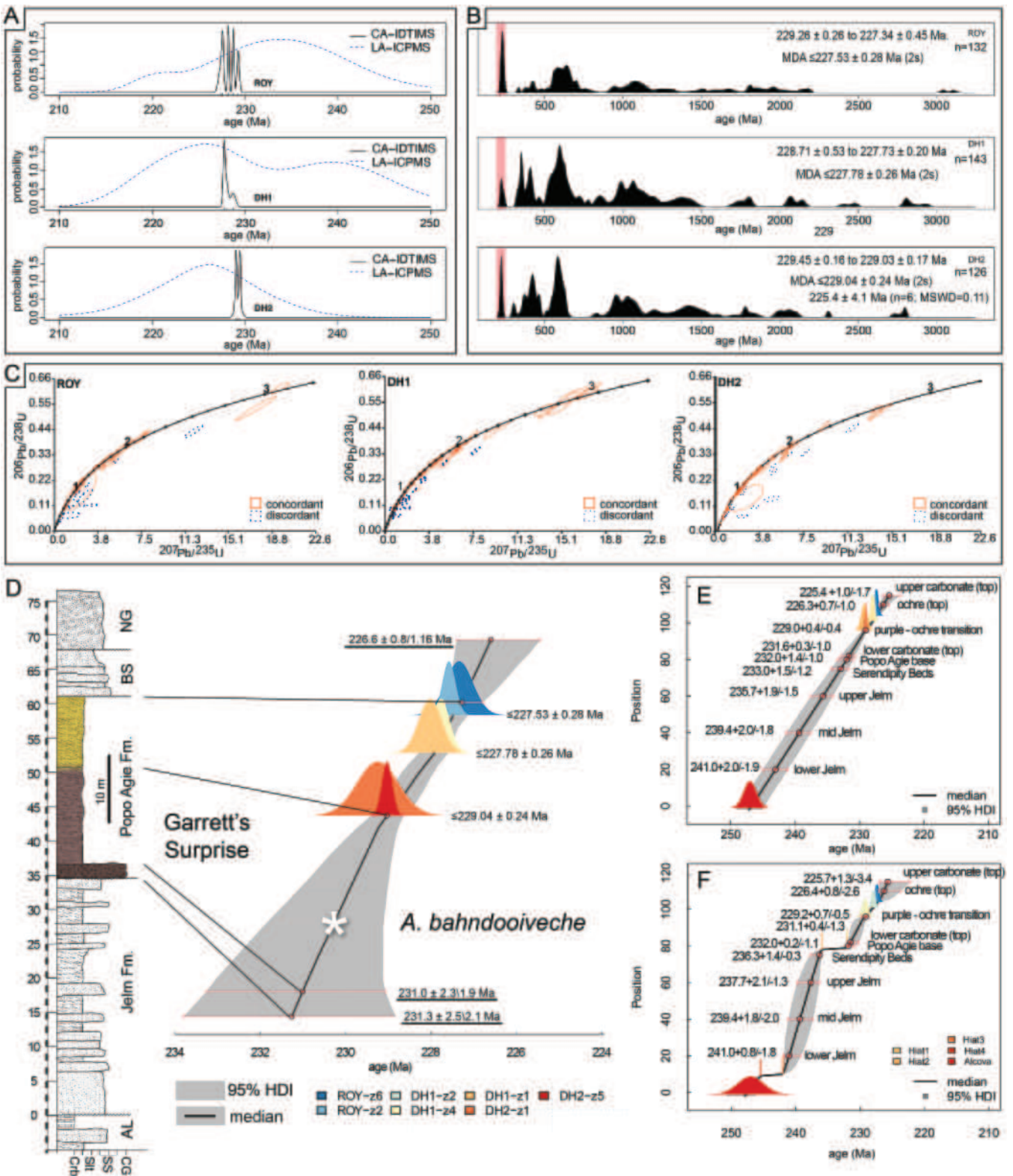


Figure 6. U-Pb radioisotopic analyses of detrital zircons are represented as probability density plots (A) comparing tandem LA-ICP-MS and CA-ID-TIMS maximum depositional age results, kernel density estimates (B) with the youngest population highlighted (shaded bar), and concordia plots (C) for three samples (LA-ICPMS). Stratigraphic profile of Garrett's Surprise (D) tied to an age-depth model using the R package 'modifiedBchron' (Methods) with predicted boundary ages (underlined) and maximum depositional ages for the Popo Agie Formation. Additional modeled ages incorporated an age-controlled Alcova LS as an anchor without (E) and with (F) a hialal bound Jeilm Formation. AL: Alcova Limestone, BS: Bell Springs Formation, NG: Nugget Formation.

high-resolution detrital age for the fossiliferous upper Popo Agie, the age of the base is still poorly constrained with the next oldest temporal bound being the Alcova Limestone from the Early–Middle Triassic boundary (Lovelace and Doebbert 2015). Our age-depth model predicts chronostratigraphic positions for new ornithodiran material, as well as the base of the formation, under three conditions: (i) when only the Popo Agie Formation is considered in the model (Fig. 6D); (ii) with the addition of the Jelm Formation and underlying age-controlled Alcova Limestone (the next oldest age-constraint) without a hiatus (Fig. 6E); and (iii) with hiatal-bound upper and lower contacts of the Jelm Formation (Fig. 6F) following previous arguments for hiatuses (High and Picard 1967, Johnson 1993). Our age-depth model predicts an age for the base of the Popo Agie of $c. 231 + 2.5/-2.1$ Mya (95% HDI) when just the Popo Agie Formation is considered, a modelled age of $232 + 1.3/-1.2$ Mya (95% HDI) without a Jelm Formation hiatus, and $232 + 0.2/-1.1$ Mya (95% HDI) with hiatal boundaries at the top and bottom of the Jelm Formation. Based on these models, we predict a $c. 230$ Mya age for the Garrett's Surprise locality, suggesting that UWGM 1975 and UWGM 7407 are roughly equivalent to the modelled age of 230.2 ± 1.9 Mya for the base of the Ischigualasto Formation, Argentina (Desojo *et al.* 2020). Herein, we will use the more conservative age-depth model with only the Popo Agie modelled, and use the model age of $c. 231.3 \pm 2.5$ Mya for the base of the Popo Agie. The modelled age for the base of the Popo Agie is in line with the presence of *Beesiiwo coowuse* Fitch *et al.*, 2023, an early-diverging hyperodapedontine [a clade that ranges from $c. 237$ Mya to no younger than 227 Mya (Langer *et al.* 2018, Desojo *et al.* 2020)].

Histology

Our sample consists of a complete transverse section of the proximal femur taken as close to the diaphysis as possible. The preserved region of the femur dictates that our histological sample is closer to the proximal articular condyle than ideal, and we observe more trabecular bone than expected if our section had been extracted from the mid-diaphysis (Fig. 7). That said, the femur is often subjected to less intensive secondary remodelling than other appendicular and axial skeletal elements, and thus affords a valuable perspective on growth history in *Ahwaytum*. The description of bone microstructure is organized from deep to superficial, beginning with the medullary space and deep cortex, and continuing outward to the periosteal margin. We focused on primary bone mineral organization, primary vascular organization, presence/absence of growth marks (annuli, LAGs, EFS), and also document features of secondary bone remodelling (secondary osteons, trabecular formation, IFS).

The femur of *Ahwaytum* exhibits a somewhat crushed but well-defined medullary cavity with a few, sparse bony trabeculae, which extend nearly to the periosteal margin in many areas of the cross-section (Fig. 7). Where visible, the medullary cavity is lined in some areas by endosteal lamellae forming an IFS (Fig. 7C, D). These patches of thin avascular lamellar bone crosscut primary bone deposits in the deepest regions of the cortex and indicate medullary drift driven by cycles of perimedullar bone resorption and redeposition (Fig. 7D). In a few regions primary bone persists between remodelled trabeculae, and a few

large erosion rooms and sparse secondary osteons are present (Fig. 7C, D). The primary femoral cortex is very thin but visible in the anterior and lateral regions of the cross-section where fibrolamellar bone is dominated by longitudinally oriented primary osteons and abundant osteocyte lacunae (Fig. 7C, E). In a few regions, reticular and radial primary osteons are oriented in the direction of the head of the femur (Fig. 7A, B). Though only a few narrow zones of primary bone tissue persist, they are devoid of annuli and LAG (Fig. 7A–C, E, F). At the periosteal surface, the element records a shift toward a more organized growth pattern, with a transition parallel and lamellar fibred primary bone tissue that includes flattened osteocyte lacunae arranged in thin, parallel layers, and very limited primary osteons (Fig. 7E). Where present, these osteons are longitudinal and relatively constricted compared to deeper regions of the cortex. There is no EFS at the external margin of the element (Fig. 7E, F), indicating that skeletal maturity had not been obtained, though peripheral shifts in primary bone tissue organization are consistent with slowing appositional growth at the time of death.

Phylogenetic position

Preliminary phylogenetic results recovered *Ahwaytum bahndooiveche* (UWGM 1975 and UWGM 7549), combined with indeterminate dinosauro-morph elements (UWGM 7434) and the distal end of a silesaurid humerus (UWGM 7550) misidentified as a proximal metatarsal III, as a non-neotheropod theropod (Fitch *et al.* 2020). However, in the presented analyses *A. bahndooiveche* is consistently recovered with *Eoraptor lunensis* and *Buriolestes schultzi* as a sauropodomorph or as an early diverging saurischian. UWGM 7407 is recovered as a sulcimentisaurian silesaurid sometimes sister to *Silesaurus opolensis*.

Maximum parsimony analyses in TNT resulted in two strict consensus trees with resampling and Bremer supports: one for the combined OTU matrix (Fig. 8: 66 MPTs, 1335 steps, CI = 0.230, RI = 0.603) and one for the split OTU matrix (Supporting Information, Fig. S2 in Text S1): 66 MPTs, 1334 steps, CI = 0.224, RI = 0.590). Silesaurids, including UWGM 7407, are recovered in a polytomy along with Ornithischia and Saurischia. *Saltopus elginensis* von Huene, 1910 is recovered as the earliest diverging saurischian with weak support, and the remainder of Saurischia includes Herrerasauria as an early-diverging clade of saurischians and Theropoda and Sauropodomorpha as sister-taxa. Exclusion of *S. elginensis* resulted in no significant change in the resolution of tree topology, so it was retained in all analyses despite often being excluded in several previous analyses due to incompleteness. In the split OTU analysis, the holotype and referred specimens of *A. bahndooiveche* are recovered in slightly different positions among the earliest diverging sauropodomorphs. The astragalus is consistently recovered in a weakly-supported polytomy with *E. lunensis* and *Bu. schultzi*, but the referred femur is recovered in a polytomy at the base of Sauropodomorpha, along with saturnaliids, *Mbiresaurus raathi*, and *Bagualosaurus agudoensis*. In the combined OTU analysis, *A. bahndooiveche* is recovered as a member of a weakly-supported and more inclusive Saturnaliidae in a clade with *M. raathi*, *E. lunensis*, and *Bu. schultzi*.

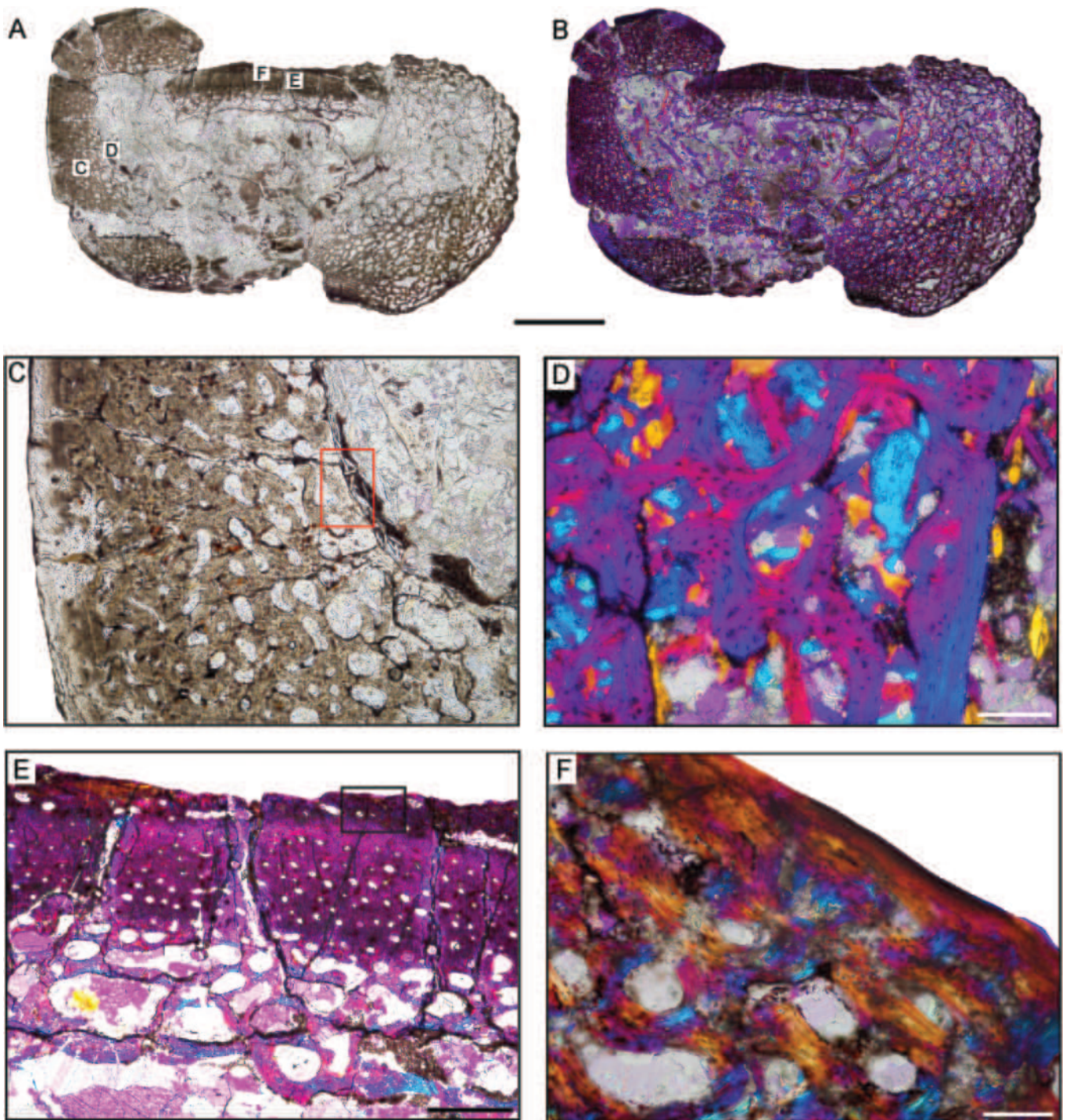


Figure 7. Femoral histology of *Ahvaytum bahndooiveche* UWGM 1975 General view of femoral histology in (A) plane polarized light (PPL) and (B) cross-polarized light with a lambda compensator (XPL). Letters in (A) indicate positions of higher magnification photomicrographs (C–F). Anterior is toward the top in (A–B). Scale bar = 1 mm. C, PPL image of a thin, highly vascularized cortex (left) that surrounds an open medullary space (right) surrounded by thin bony trabeculae. Fibrolamellar primary cortical bone tissue is vascularized by irregular reticular and longitudinal primary osteons with occasional radial anastomoses. Scale bar = 500 microns. Rectangle indicates position of image (D). D, XPL image highlighting secondary bone remodeling in the deep cortex indicated by the Internal Fundamental System (IFS). The IFS consists of layers of centripetally deposited, avascular lamellar fibered bone (LFB) lining the open medullary cavity. Scale bar = 300 microns. E, XPL image documenting the external primary cortex. Most of the preserved primary cortex is well vascularized fibrolamellar bone, dominated by longitudinal primary osteons with occasional circular anastomoses. A transition to more poorly vascularized lamellar fibered bone characterizes the most external cortex. Black rectangle indicates position of image (F) Scale bar = 500 microns. F, XPL image of the most superficial cortex. In this image the woven bone component of the fibrolamellar complex is indicated by pinker regions, while more organized LFB surrounds primary osteons, is layered at the periosteal surface, and is indicated by turquoise and orange regions. Scale bar = 150 microns.

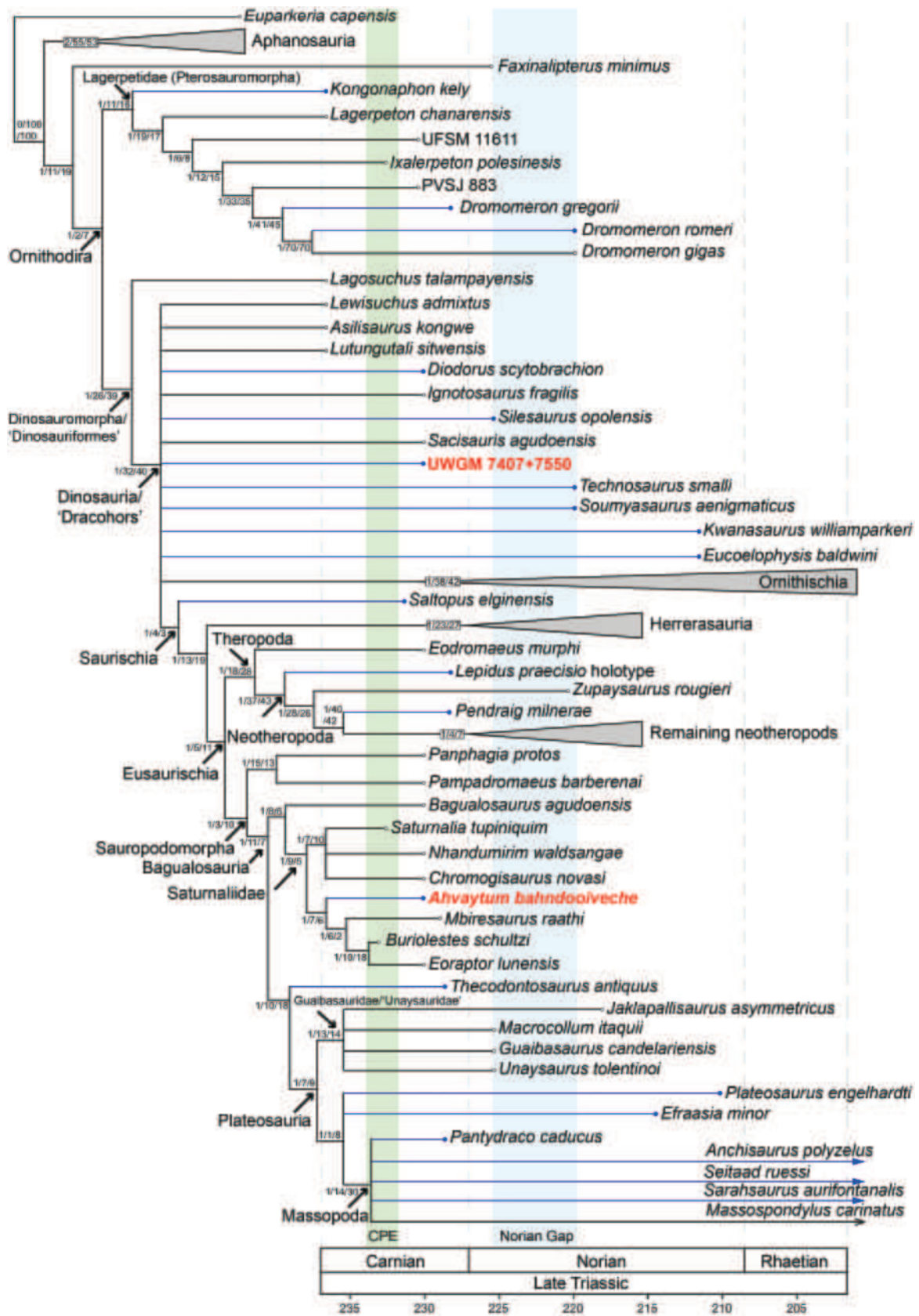


Figure 8. Strict consensus tree of avemetatarsalians and *Euparkeria capensis* using the combined OTU of *Ahvaytum bahndooiveche* obtained through maximum parsimony implemented in TNT v.1.5. The shaded interval (left) is the approximate duration of the Carnian Pluvial Episode (CPE), and the shaded interval (right) is the ‘Norian gap’ in the dinosaur record. Branches with filled in dots indicate northern hemisphere taxa and branches with hollow dots indicate southern hemisphere taxa. Dots at the end of branches are the approximate earliest occurrences of each taxon. For any higher taxon labels with two names, the latter name represents a widely used taxon that in the current analyses would be a junior synonym of the former. Statistical support values at nodes are: Bremer support decay indices/bootstrap resampling/jackknife resampling. All nodes with resampling values less than 15 indicate low support. *Ahvaytum bahndooiveche* and UWGM 7407+7550 are indicated in bold text.

The Bayesian trees differ from the parsimony trees with several typically non-sulcimentisaurian silesaurids recovered in a polytomy with the clades of Saurischia and Sulcimentisauria, inclusive of Ornithischia and UWGM 7407. Sometimes UWGM 7407 is recovered as the sister-taxon of *S. opolensis*, although this placement is only recovered in the Bayesian analyses and moderately supported (~ 0.5 PP) (Fig. 9; Supporting Information, Figs S3, S4 in Text S1). The phylogenetic position of *A. bahndooiveche* in the Bayesian analyses is similar to the parsimony analyses, but the early sauropodomorphs were recovered in a polytomy at the base of Saurischia (Fig. 9) with weak support in the fully bifurcated tree for a theropod placement of *E. lunensis*, *Bu. schultzi*, *M. raathi*, and *A. bahndooiveche* (see Supporting Information, Fig. S3 in Text S1). In the split OTU analysis, the holotype astragalus is moderately well-supported as the sister-taxon of *E. lunensis* (0.64 PP). The clade of ‘*Eoraptor* + *Ahvaytum* holotype’ is found in a polytomy at the base of Saurischia (Supporting Information, Fig. S4 in Text S1), including saturnaliids, *Bu. schultzi*, and Bagualosauria (Langer *et al.* 2019). The referred femur is also recovered in this polytomy at the base of Saurischia and weakly supported as the earliest diverging member of Saturnaliidae in the fully bifurcated summary tree (Supporting Information, Fig. S4 in Text S1). The combined OTU of *Ah. bahndooiveche* is recovered in this polytomy along with *Bu. schultzi*, *E. lunensis*, *Panphagia protos*, *Pampadromaeus barberenai*, and *M. raathi* (Fig. 9).

DISCUSSION

Phylogenetic implications

The recovery of *Ahvaytum bahndooiveche* as an early-diverging saurischian and probable sauropodomorph in the post-CPE Carnian of Wyoming, USA demonstrates a more rapid dispersal of dinosaurs into lower latitudes and the northern hemisphere than previously recognized. However, the instability of the relationships between the clades of Dinosauromorpha has been a matter of recent discussion (Baron *et al.* 2017, Langer *et al.* 2017), and it warrants further consideration for the phylogenetic placement of fragmentary taxa such as *A. bahndooiveche* and UWGM 7407, and any inferences therein. Our analyses recovered *A. bahndooiveche*, *Eoraptor lunensis*, *Buriolestes schultzi*, and other early-diverging forms that are commonly included among sauropodomorphs as early-diverging saurischians with weak support for theropod affinities of these taxa in the Bayesian analyses. We consider this to be due (at least in part) to character sampling bias as there are 304 characters in the present analysis compared to other recent analyses of early dinosaurs with 388 (Spiekman *et al.* 2021) and 419 characters (Pol *et al.* 2021), respectively. Some derivations of the matrix of Baron *et al.* (2017) have also recovered *E. lunensis* as a theropod (Langer *et al.* 2017) or an unresolved saurischian (Nesbitt *et al.* 2020a). However, Spiekman *et al.*'s (2021) phylogenetic analysis of early dinosaurs, with 84 additional characters but a lower taxon sample than our study (e.g. five sauropodomorphs compared to 20), recovered a well-supported Sauropodomorpha inclusive of *E. lunensis* and *Bu. schultzi*, while Kirmse *et al.* (2023) [using the matrix of Spiekman *et al.* (2021)] recovered *E. lunensis* and *Bu.*

schultzi in an unresolved polytomy at the base of Saurischia. Additionally, Ezcurra *et al.* (2023) recovered several topologies of Sauropodomorpha differing most in the positions of early-diverging taxa with weak support for *E. lunensis* and *Bu. schultzi* as early-diverging sauropodomorphs using a modified version of the sauropodomorph-dominated character matrix of Yates (2007). The analyses of Müller and Garcia (2020), Norman *et al.* (2022), and Garcia *et al.* (2023), from which our matrix was derived, all recovered *E. lunensis* and *Bu. schultzi* as sauropodomorphs. Although the issue of early saurischian phylogeny has not reached consensus, and regardless of its precise phylogenetic position within Saurischia, *A. bahndooiveche* is unequivocally the oldest known low-latitude dinosaur and one of the oldest in the northern hemisphere.

Similarly, phylogenetic relationships between Silesauridae and core Ornithischia continue to be unstable and have been the focus of numerous analyses (Langer and Ferigolo 2013, Müller and Garcia 2020, 2023, Nesbitt *et al.* 2020a, Norman *et al.* 2022). Two phylogenetic scenarios found herein, and with similar results in previous studies (e.g. Cabreira *et al.* 2016, Mestriner *et al.* 2023), result in Dinosauria inclusive of non-monophyletic ‘silesaurids’ and are hereafter referred to in single quotations to reflect this uncertainty in their monophyly. In our analyses, ‘silesaurids’ are recovered in unresolved polytomies in two ways: (i) Dinosauria includes all ‘silesaurids’ in a polytomy with core Ornithischia and Saurischia (inclusive of *Saltopus elginensis*) (Fig. 8) and (ii) Dinosauria includes a polyphyletic ‘Silesauridae’ with non-sulcimentisaurians, Sulcimentisauria + core Ornithischia, and Saurischia in a polytomy (Fig. 9). UWGM 7407 was consistently recovered in this polytomy among ‘silesaurids’ with moderately well-supported sulcimentisaurian affinities in our analyses. Previous iterations of the matrix used in our study (Müller and Garcia 2020, Norman *et al.* 2022, Garcia *et al.* 2023) and others (e.g. Fonseca *et al.* 2024) have recovered a paraphyletic ‘Silesauridae’ with respect to Ornithischia. Others have found a sister-relationship between a monophyletic Silesauridae and Dinosauria referred to as Dracohors (Cau 2018, Ezcurra *et al.* 2020a, Nesbitt *et al.* 2020a, Spiekman *et al.* 2021), and still others have recovered a sister-relationship between Sulcimentisauria and core Ornithischia (Cabreira *et al.* 2016). Further efforts to clarify the relationships of ‘silesaurids’ among Dinosauromorpha are needed to resolve their phylogenetic position relative to Dinosauria. The resolution of this relationship has significant implications for the evolution and taxonomy of the stem-avian lineage, e.g. rendering Dinosauriformes a junior subjective synonym of Dinosauromorpha.

The discoveries of ‘silesaurids’ such as *Lutungutali sitwensis* (Peacock *et al.*, 2013), *Gamatavus antiquus* (Pretto *et al.*, 2022), and *Asilisaurus kongwe* (Nesbitt *et al.*, 2010a) have pushed the origins of an inclusive Dinosauria into the Ladinian or at the latest the Ladinian–Carnian boundary (Müller and Garcia 2023). The distribution of other early Late Triassic ‘silesaurids’ from mid–late Carnian strata are roughly split between the southern [i.e. *Amanasaurus nesbitti* (Müller and Garcia, 2023), *Ignotosaurus fragilis* (Martinez *et al.*, 2012), and *Sacisaurus agudoensis* (Ferigolo and Langer, 2007)] and northern hemispheres [i.e. *Diodorus scytobranchion* (Kammerer *et al.*, 2012) and UWGM 7407].

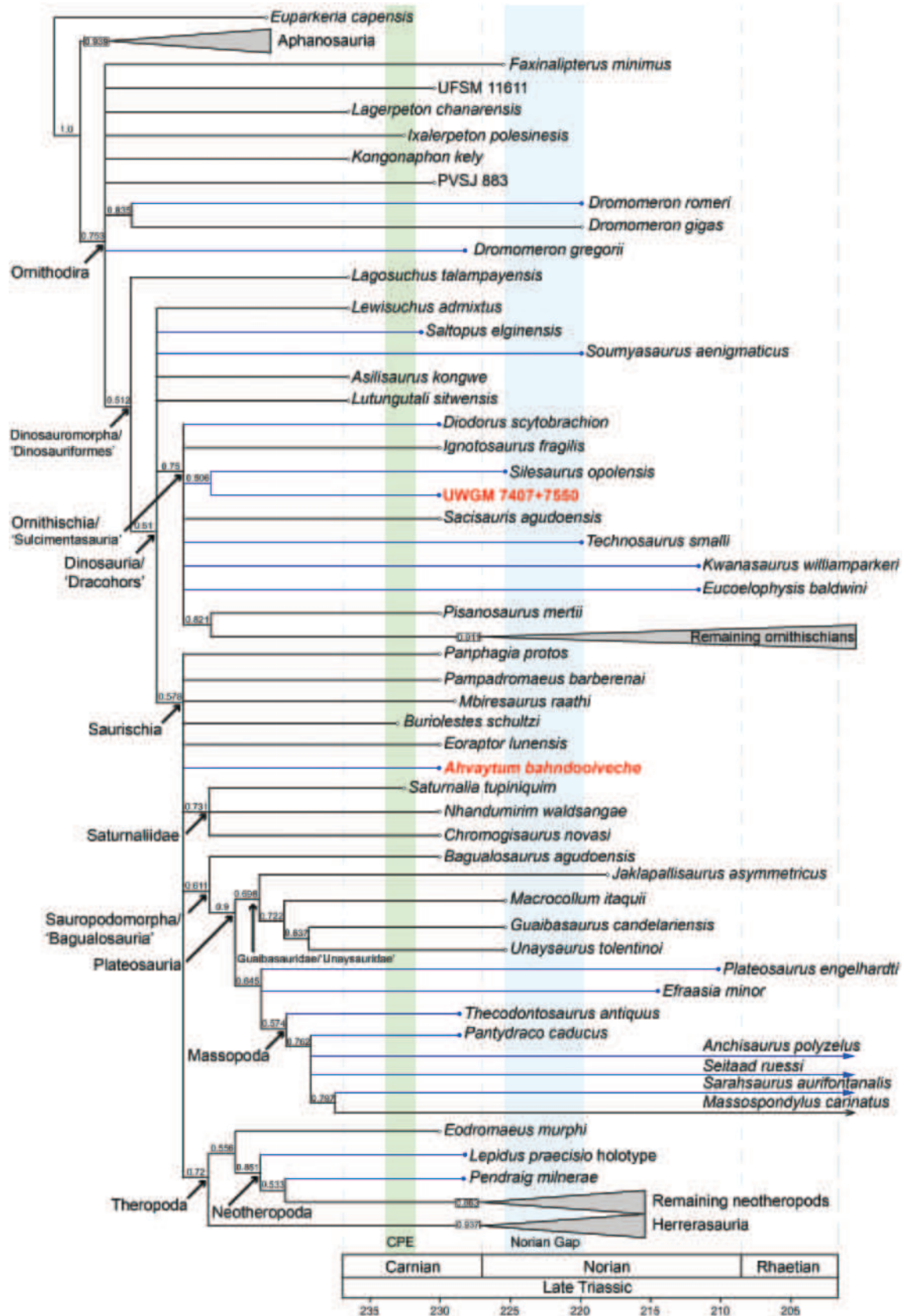


Figure 9. Consensus tree of avemetatarsalians and *Euparkeria capensis* using the combined OTU of *Ahvaytum bahndooiveche* obtained through Bayesian inference implemented in MrBayes v.3.2.6. The shaded interval (left) is the approximate duration of the Carnian Pluvial Episode (CPE), and the shaded interval (right) is the 'Norian gap' in the dinosaur record. Branches with filled in dots indicate northern hemisphere taxa and branches with hollow dots indicate southern hemisphere taxa. Dots at the end of branches are the approximate earliest occurrences of each taxon. For any higher taxon labels with two names, the latter name represents a widely used taxon that in the current analyses would be a junior synonym of the former. Statistical support values at nodes are posterior probabilities. All nodes with posterior probability < 0.5 were considered poorly supported and thus collapsed. The fully bifurcated tree can be found in [Supporting Information, Fig. S3 in Text S1](#). *Ahvaytum bahndooiveche* and UWGM 7407+7550 are indicated in bold text.

The results of our phylogenetic analyses and most recent analyses suggest a deeper origin of Dinosauria that extends into the Ladinian or, at a minimum, the Ladinian–Carnian boundary based on the oldest unequivocal ‘silesaurid’ body-fossils (Müller and Garcia 2022). Our results also suggest that all three major dinosaur lineages (Ornithischia, Sauropodomorpha, and Theropoda) either had a cosmopolitan distribution prior to the CPE or underwent a more synchronous dispersal during the CPE than previously recognized. Similar faunal associations of ‘silesaurids’ and early saurischians have been found in the Ischigualasto Formation in Argentina (Martínez *et al.* 2012) and the Candelária Sequence in Brazil (Garcia *et al.* 2023), and now, the Popo Agie Formation of the USA. Unfortunately, a poor Middle Triassic terrestrial fossil record globally, and an absence of aged-controlled strata of similar age in North America (Dubiel 1994, Lovelace 2012), inhibit spatiotemporal faunal comparisons beyond the Carnian of the northern hemisphere at this time.

Northern hemisphere Carnian-aged dinosaurs

Over the last decade high-resolution radioisotopic ages have greatly improved Late Triassic chronostratigraphy placing temporal constraints on palaeobiogeographic distributions, geological events such as the CPE, and the early evolution of dinosaurs and their closest relatives (Marsicano *et al.* 2016, Langer *et al.* 2018, Philipp *et al.* 2018, Dal Corso *et al.* 2020, Desojo *et al.* 2020, Simms and Drost 2024). Age-depth models of stratigraphically stacked radioisotopic ages have resulted in several chronostratigraphic hypotheses of global correlations (Desojo *et al.* 2020, Rasmussen *et al.* 2020). Our own age-depth hypotheses tied to CA-ID-TIMS ages restrict the dinosaur-bearing lower Popo Agie Formation to *c.* 231–229 Mya, i.e. mid–late Carnian Stage, *sensu* Cohen *et al.* (2013) making this unit analogous to the oldest dinosaur-bearing strata globally (Langer *et al.* 2018, Desojo *et al.* 2020, Griffin *et al.* 2022).

Our temporal constraints for the lower Popo Agie Formation (see above) have direct implications for the age of other North American strata. Lovelace *et al.* (2024) proposed a chronostratigraphic correlation between the Camp Springs Conglomerate and conglomerates at the base of the Popo Agie Formation (i.e. Gartra Grit, lower carbonate unit) based on multidimensional scaling statistical analyses of detrital zircon age distributions from throughout the Late Triassic of the western USA. This is further supported by comparable Otischalkian (*sensu* Martz and Parker 2017) faunal components in both the lowermost Dockum Group and the Popo Agie Formation (Lovelace *et al.* 2024). As such, the classic Otis Chalk localities, including the early-diverging neotheropod *Lepidus* from the Colorado City Formation (lower Dockum Group), can be restricted to somewhere between the late Carnian (*c.* 231 Mya; this study) to no younger than early Norian [*c.* 221 Mya; (Nesbitt and Ezcurra 2015, Lovelace *et al.* 2024)]. Other temporally comparable terrestrial strata from the northern hemisphere have been previously reported from North America (Olsen *et al.* 2010, Sues and Olsen 2015, Sues *et al.* 2020), Europe (Milroy *et al.* 2019, Zeh *et al.* 2021, Simms and Drost 2024), and West Africa (Tourani *et al.* 2023).

Due to a significantly older shift in the chronostratigraphic position of the Carnian–Norian boundary (Cohen *et al.* 2013),

caution should be exercised when considering units and their correlatives historically reported to be mid-Carnian in age (Porchetti *et al.* 2008, Kozur and Weems 2010, Bernardi *et al.* 2013, Geyer and Kelber 2018). Stratigraphic units such as the Weser Formation (Germany), Travenanzes Formation (Italy), and the lower Grabowa Formation (Poland) are now considered very late Carnian to early Norian (Olsen *et al.* 2010, Szulc *et al.* 2015, Menning *et al.* 2022).

Additionally, dinosaur-bearing strata from the Late Triassic ‘fissure’ fill deposits of Britain, thought to be Rhaetian (Whiteside *et al.* 2016), have recently been reinterpreted to be dominantly Carnian in age (Simms and Drost 2024). Simms and Drost (2024) demonstrate that the Late Triassic fill deposits along the Bristol Channel (southern Britain) are more complex than typically considered. Their compelling argument indicates the majority of sediment that filled epigenic karst conduits (not fissures) formed during the CPE and are largely coeval with speleogenesis (Simms and Ruffell 1989, Simms and Drost 2024). U–Pb ages from speleothems support a mid–late Carnian age for many of the deposits (Simms and Drost 2024). As such, they consider much of the associated fill-fauna to be mid–late Carnian and suggest that it probably extends into the early Norian and not dominantly Rhaetian as reported by others (e.g. Whiteside *et al.* 2016). They point out that a Carnian age is also more consistent with the early-diverging phylogenetic positions of the sauropodomorphs *Thecodontosaurus antiquus* Riley and Stutchbury, 1836, *Pantyraco caducus* Galton *et al.*, 2007, and *Asylosaurus yalensis* Galton, 2007, and (we would suggest) possibly the neotheropod *Pendraig milnerae* Spiekman *et al.*, 2021 along with numerous other non-dinosaurian taxa (Galton and Kermack 2010, Foffa *et al.* 2014, Müller *et al.* 2018, Ballell *et al.* 2020, Spiekman *et al.* 2021). *Pe. milnerae* is often recovered as an early-diverging neotheropod (Spiekman *et al.* 2021, Kirmse *et al.* 2023) as it is in our analysis. As with previous studies we also find an early-diverging position for *T. antiquus* (Yates 2007, Baron *et al.* 2017, Langer *et al.* 2017, Pol *et al.* 2021, Ezcurra *et al.* 2023); however, the massopodan position of *Pa. caducus* is relatively derived in our analysis but is consistent with previous iterations of this matrix (e.g. Norman *et al.* 2022, Garcia *et al.* 2023, *contra* Yates 2007, Pol *et al.* 2021, Ezcurra *et al.* 2023). In addition, several of the characters that unite *T. antiquus* and *Pa. caducus*, such as the shape of the post-axial epiphyses, were not implemented in the current matrix due to difficulty in assessing these in taxa that could not be observed firsthand. The only previous phylogenetic analyses to incorporate both *T. antiquus* and *Pa. caducus* in a broader context with ornithodirans are derivations of the character matrix of Baron *et al.* (2017) with modifications of Langer *et al.* (2017) (e.g. Nesbitt *et al.* 2020a). More commonly, these taxa are included in sauropodomorph-dominated analyses looking to resolve sauropodomorph phylogeny (e.g. Yates 2007, Pol *et al.* 2021, Ezcurra *et al.* 2023). Inclusion of more Carnian taxa from deposits around the world (and potentially Carnian-aged fill deposits of Britain) could help better resolve early dinosaur relationships.

Given the new temporal constraints outlined above, there appears to be much greater taxonomic diversity and a broader palaeogeographic distribution of Carnian-aged dinosaurs than previously recognized. The presence of roughly-contemporaneous, low- to mid-latitude, small-bodied

Carnian-aged saurischians (i.e. *Ah. bahndooiveche* and *T. antiquus*; possibly *L. praecisio*, *Pe. milnerae*, *Pa. caducus*, and *As. yalensis*) from the northern hemisphere of Pangaea greatly expands the spatiotemporal range of the earliest saurischian dinosaurs and helps to address the late Carnian–early Norian gap in the early dinosaur record (Langer *et al.* 2018). It must be noted that a significant temporal gap (c. 10–15 Mya) still exists between *Ahvaytum bahndooiveche* and *T. antiquus* and the next oldest sauropodomorph body-fossils (late Norian) from the northern hemisphere (i.e. *Efraasia minor*; Yates 2003). Regardless, these taxa demonstrate a Carnian presence of small-bodied early saurischian and probable sauropodomorph dinosaurs at low to mid palaeolatitudes, rejecting a central tenet of the diachronous rise hypothesis (Irmis *et al.* 2011, Griffin *et al.* 2022).

Palaeoenvironmental barriers

The historical absence of sauropodomorphs from known low-latitude, Late Triassic deposits has been explained by large-scale inhospitable environmental barriers (Kent and Clemmensen 2021, Griffin *et al.* 2022, Dunne *et al.* 2023), resource competition (Dunne *et al.* 2021), and strong mid–late Late Triassic seasonal fluctuations and environmental instability (Whiteside *et al.* 2015); restrictions that may have led to regional endemism (Button *et al.* 2017, Griffin *et al.* 2022). Physiological niche models hypothesized hot low-latitude climates would have been unsuitable for larger-bodied sauropodomorphs, though smaller forms were predicted to be viable (Lovelace *et al.* 2020, Hartman *et al.* 2022).

Although climatic barriers certainly existed, figures illustrating ‘dry’ climate belts extending across the entirety of mid-latitudes during the Carnian (Kent and Clemmensen 2021, Griffin *et al.* 2022) may be an oversimplification of a complex system. General circulation models (GCMs) incorporate multiproxy datasets in order to predict mean annual temperature (MAT) and precipitation (MAP), and hypotheses resulting from Triassic-focused GCMs (Sellwood and Valdes 2006, Dunne *et al.* 2021) suggest higher MAP along the eastern Tethyan coast. This is further supported by outcrop and core data such as the prevalence of koalanitic palaeosols (Khalifa 2007, Bourquin *et al.* 2010); however, outcrops of terrestrial strata along the Tethyan coast are rare, limiting their contribution to the vertebrate fossil record. Based on the GCM-derived Carnian MAP/MAT model (Dunne *et al.* 2021), we suggest that coastal areas along the eastern margin of Pangaea may have been more persistently wet (or humid), allowing greater connectivity between the hemispheres than previously thought (Fig. 10).

Palaeoclimates play a significant role in the total range of many clades, which can be observed in the spatial distribution of water-bound taxa such as Phytosauria and Metoposauridae (Fig. 10G; Lee *et al.* 2018, Dunne *et al.* 2021, 2023). These clades largely follow areas with higher MAP across low-latitude Laurasia and down the eastern Tethyan seaboard into high-latitude Gondwana; however, their absence in the Carnian (and rarity in the Norian of the Paraná; Kischlat and Lucas 2003) of the Paraná and Ischigualasto basins may be a result of smaller scale palaeoclimatic barriers (i.e. low MAP) as a result of their mid-high latitude positions far inland from the eastern Tethyan coast (Sellwood and Valdes 2006, Colombi *et al.* 2021, Dunne

et al. 2021). Although Dunne *et al.* (2021) could not confirm a relationship between species’ richness and palaeoclimatic conditions, sampling was proposed to be the primary driver of apparent latitudinal distributions in most cases.

Low latitudes (0–30°) of the southern hemisphere are not represented in tetrapod-bearing collections (Dunne *et al.* 2021). In addition, poor sampling from low latitude northern hemisphere early Late Triassic strata has probably played a role in perceived latitudinal barriers (Kent and Clemmensen 2021, Griffin *et al.* 2022). However, sampling bias in tetrapod-bearing collections is contingent on many factors that affect collection efforts (e.g. ease of access, permissions, and funding) or geological contingencies (e.g. active margins, rifts, orogenic belts, and cratonic interiors) that affect where and when accommodation and sediment supply will allow for long-term preservation of sedimentary deposits.

Surficially-expressed stratigraphic occurrences observed in the Macrostrat database (macrostrat.org) match well with the spatiotemporal distribution of fossils in the Paleobiology Database (PBDB; paleobiodb.org), demonstrating that fossil occurrences can act as a proxy for accessible outcrops (Ye and Peters 2023). This can readily be seen when mappable Triassic strata from Macrostrat (Fig. 10C) are plotted alongside PBDB fossil occurrences (Fig. 10D–F). These data show that the vast majority of accessible Gondwanan outcrops are from mid-high palaeolatitudes with a notable paucity of mid- to low-latitude stratigraphic occurrences (cratonic interiors). These stratigraphic ‘voids’ impart a bias that is reflected in palaeontological sampling contributing to the false appearance of latitudinally controlled species’ richness and distribution, a suggestion forwarded by Dunne *et al.* (2021).

Vertebrate clades typical of early Late Triassic dinosaur-bearing faunas appear to have a rather cosmopolitan distribution suggesting significant biotic communication throughout the early Late Triassic (Fig. 10B), rejecting a more ‘centres of origin’ perspective. With the addition of *Ahvaytum bahndooiveche* and the probable mid–late Carnian age of *Thecodontosaurus antiquus* and possibly *Lepidus praecisio*, *Pantydraco caducus*, *Pendraig milnerae*, and *Asylosaurus yalensis*, the origin of dinosaurs is more complex than currently recognized. Additional efforts and other novel research in less-productive Carnian intervals of the northern hemisphere should be integral to further elucidate stem-avian origins and the evolution of Dinosauria.

Hidden vertebrate biodiversity

There is a long history of vertebrate trace fossils preceding the first occurrence of corresponding tracemaker body-fossils (Niedźwiedzki *et al.* 2010, Brusatte *et al.* 2011, Lovelace and Lovelace 2012, Bernardi *et al.* 2015, Lichtig *et al.* 2018, Edgar *et al.* 2023). It should be noted that most studies of early dinosaur evolution do not include, or only allude to, the vertebrate ichnological record, potentially exaggerating the absence of various clades with some exceptions (e.g. Marsicano *et al.* 2007, Bernardi *et al.* 2018). Traces are often preserved in depositional settings that limit body-fossil preservation, expanding the probability of recording the presence of a particular clade at a given time, i.e. hidden biodiversity (Hasiotis 2007, Lovelace and Lovelace 2012). We acknowledge that vertebrate traces are

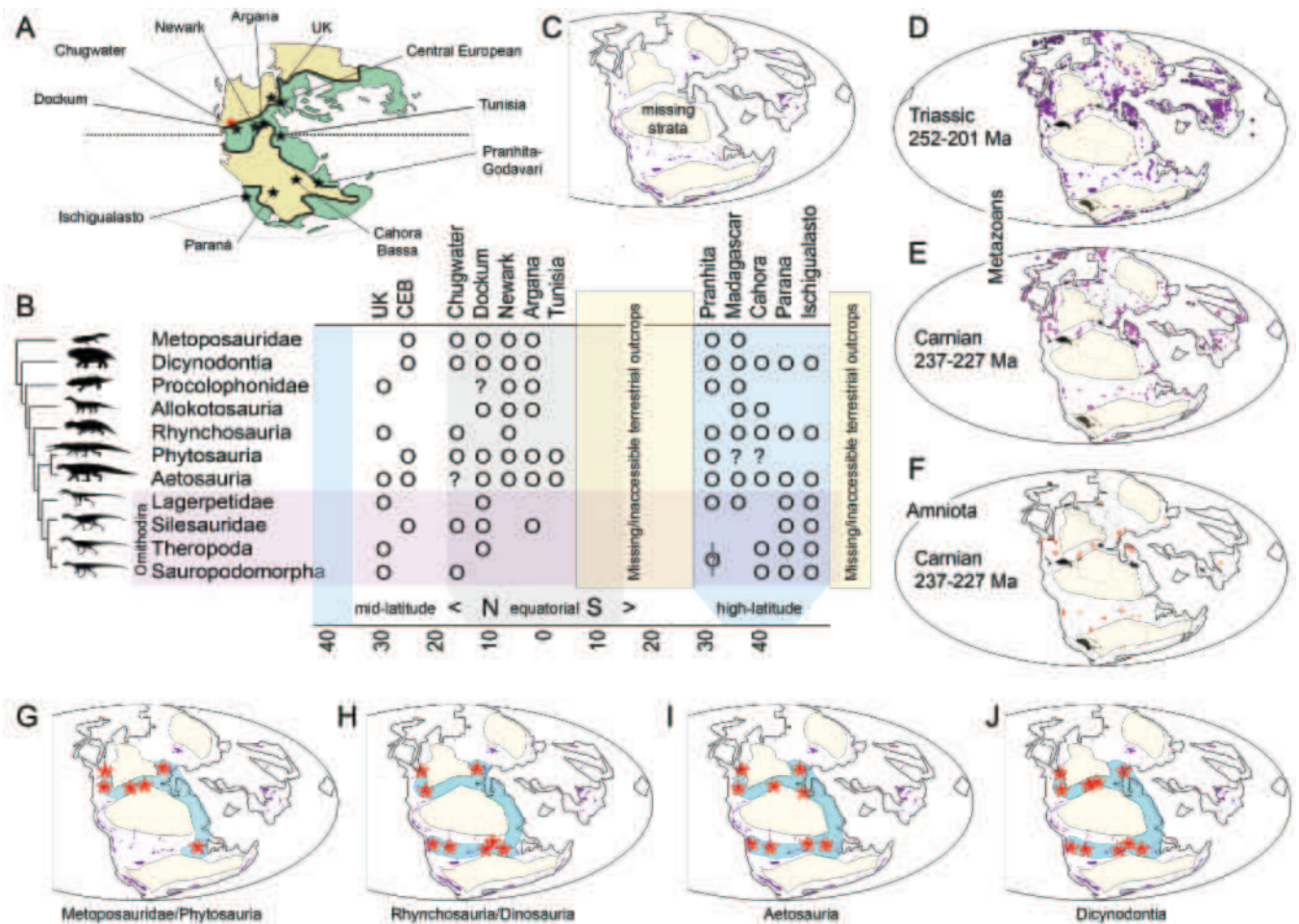


Figure 10. Paleogeography of 12 Pangaeen basins with Carnian-aged vertebrate assemblages (A) and the relative distribution of 11 clades (B) across north and south latitudes. Areal representation of Triassic strata exposed at Earth's surface (macrostrat.org) (C) coincides with the total metazoan record for the entire Triassic (D), only the Carnian (E), and the Carnian amniote record (F). (PaleobioDB.org; accessed Feb, 2024; [Supporting Information, Data S1](#)). Four palaeobiogeographic maps demonstrate the spatial distribution of amniote clades that are: largely water bound (G), small bodied (H), or large bodied forms (I, J). Circles = present, blank = unknown, ? = uncertainties exist (age control, taxonomic status, etc.). Silhouettes from Phylopic.org; credits provided in [Supporting Information, Text S1](#).

an imperfect representation of tracemakers and have a more broadly focused applicability relative to body-fossils, but traces are an integral part of the fossil record and should be considered in any palaeobiogeographic study that includes presence or absence data for support. Vertebrate traces such as *Atriepus* and *Grallator* have been strongly correlated with dinosauromorphs (i.e. silesaurids) and theropod dinosaurs, respectively (for review, see: [Klein and Lucas 2021](#)); though not all agree that *Atriepus* is an exclusively ornithodiran trace ([Farlow et al. 2014](#)).

Prior to the CPE, ornithodirans are well represented in the body-fossil record of the southern hemisphere [e.g. *Lagerpeton chanarensis* [Romer, 1971](#), *Lewisuchus admixtus*, *Lagosuchus talampayensis* [Romer, 1971 sensu Agnolin and Ezcurra \(2019\)](#), *Asilisaurus kongwe*, *Lutungutali*, and *Gamatavus*], are present globally by the late Carnian (e.g. *Saltopus elginensis*, *Diodorus scytobranchion*, UWGM 7407, and *Dromomeron gregorii* [Nesbitt et al., 2009](#)), and persist throughout the remainder of the Triassic ([Langer et al. 2013](#)). Although ornithodiran body-fossils are currently unknown from the pre-CPE northern hemisphere, there are several occurrences of time-equivalent ichnotaxa throughout

Pangaea whose tracemakers are considered to be ornithodirans, e.g. *Rotodactylus* [Peabody, 1948](#), *Atriepus*, and *Grallator* ([Haubold and Klein 2000](#), [Marsicano et al. 2007](#), [Brusatte et al. 2011](#), [Klein et al. 2011](#), [Bernardi et al. 2015, 2018](#), [Zouheir et al. 2020](#)).

UWGM 7435 represents the oldest tridactyl track referable to the *Atriepus–Grallator* plexus in North America and demonstrates the presence of at least one dinosauromorph taxon prior to Popo Agie deposition (i.e. >c. 232 Mya; [Fig. 5](#)). Similar Laurasian pre-CPE Carnian-aged *Atriepus–Grallator* traces have been documented in the Alegal Member of the Timezgadiouine Formation of Morocco ([Zouheir et al. 2020](#)) and the Grabenfield (Benk) Formation, Germany ([Haubold and Klein 2000, 2002](#)). *Grallator* traces ([Klein et al. 2011](#)) have been reported from the Irohalene Member, which is thought to have been deposited during the CPE ([Tourani et al. 2023](#)); these strata are of comparable equatorial palaeolatitude and faunal composition to the oldest dinosaur-bearing faunas globally (see [Fig. 1](#)).

The temporal gap between the oldest dinosaur body-fossils from the southern hemisphere and their first occurrences

north of the equator ranges well into the Norian >c. 221 Mya (Nesbitt and Ezcurra 2015) for theropods, and c. 215 Mya for sauropodomorphs (Kent and Clemmensen 2021). Although inhospitable climatic barriers are thought to be responsible for disparity in theropod and sauropodomorph northern radiation (Griffin *et al.* 2022, Dunne *et al.* 2023), *Atreipus*–*Grallator* and *Evazoum* Nicosia and Loi, 2003 ichnotaxa—referred to theropod and sauropodomorph tracemakers, respectively—are known from late Carnian (Haubold and Klein 2000, 2002, Nicosia and Loi 2003, Gand and Demathieu 2005, Lockley and Lucas 2013, Lockley *et al.* 2024) to the earliest Norian strata (Porchetti *et al.* 2008, Bernardi *et al.* 2013, Lockley *et al.* 2024) of North America, Italy, Germany, and France. The near-absence of sauropodomorph body-fossils from equatorial regions may be linked to environmental preferences that promote ichnofossil preservation rather than body-fossil preservation (Lovelace *et al.* 2020, Dunne *et al.* 2023, Krone *et al.* 2024), with rare exceptions such as *Ahvaytum bahndooiveche*.

CONCLUSION

The paucity or lack of recognition of Carnian-aged strata in the northern hemisphere has hindered the ability to test dispersal hypotheses of early Late Triassic faunas leading to ‘centres of origin’ hypotheses. New high-resolution radioisotopic detrital ages constrain the dinosaur-bearing lower Popo Agie Formation to the mid–late Carnian, providing a rare window into terrestrial environments of equatorial Pangaea during this time. *Ahvaytum bahndooiveche* is unequivocally the oldest known low-latitude dinosaur globally and casts doubt on proposed limits to the dispersal potential of early sauropodomorphs. In addition, the ‘silesaurid’ UWGM 7407 demonstrates the presence of other dinosauroforms (possibly early-diverging ornithischians) in this fauna. The inclusion of the Carnian ichnological record—including new tridactyl traces from the upper Jelm Formation—along with body-fossils of multiple dinosaur lineages and non-dinosauroform taxa, demonstrate a comparable vertebrate fauna throughout equatorial and mid-latitude Laurasia, and high-latitude Gondwana during or just after the CPE. This suggests a relatively cosmopolitan distribution of dinosauroforms throughout the mid–late Carnian, rather than a delayed equatorial and northern hemisphere dispersal as previously thought.

SUPPLEMENTARY DATA

Supplementary data are available at *Zoological Journal of the Linnean Society* online.

ACKNOWLEDGEMENTS

We would like to express our gratitude to the innumerable people who have helped work the Popo Agie Formation with us over the last 11 years, including the 2013–2024 UWGM field crews, Rich Slaughter, Brooke Norsted, Carrie Eaton, and all of our colleagues too numerous to name individually who have contributed to the dialogues that have informed us. Thanks to Chris Sagebiel, Jessie Maisano, and Mathew Colbert (University of Texas High-Resolution X-ray

CT Facility) and April Neander (University of Chicago PaleoCT; RRID:SCR_024763) for μ CT scanning specimens. The Wyoming Game and Fish Department’s contribution to permitting fieldwork is greatly appreciated. Thanks to C.T. Griffin for providing access to specimens of *Mbiresaurus raathi*, R.T. Müller for providing access to specimens of *Macrocollum itaquii*, Steve Lovelace, Michelle Stocker, Jann Nassif, and Garrett Johnson for field assistance, and Sterling Nesbitt for early discussions. Thanks to Brandon Price for preparation of UWGM 7407 and to Yulong Wang for 3D digital segmentation of TxVP41936-1. Special thanks to Randy Nagitsy for assistance coordinating early partnerships between the Fort Washakie Schools and ESTHPO and the UWGM, and to Aaron Bird Bear for facilitating introductions with ESTHPO and NATHPO.

CONFLICT OF INTEREST

The authors declare that they have no conflicts of interest in relation to this work.

FUNDING

D.S. and M.S. acknowledge funding for the analytical infrastructure of the Boise State Isotope Geology Laboratory through NSF grants EAR-1735889 and EAR-1920336. D.M.L. acknowledges the Friends of the Geology Museum, and the Sherry Lesar Fund for Geological Wonder for financial support.

DATA AVAILABILITY

In addition to data made available through supplementary files hosted by the *Zoological Journal of the Linnean Society* online, tomographic scan data and images are available on Morphosource for UWGM 1975 (000607569), 7549 (000607572), 7407 (000697337), 7550 (000697345), 7435 (000607578), TxVP41936-1 (000606624), and histological images of UWGM 7549 (000607948).

REFERENCES

- Agnolin FL, Ezcurra MD. The validity of *Lagosuchus talampayensis* Romer, 1971 (Archosauria, Dinosauriformes), from the Late Triassic of Argentina. *Breviora* 2019;**565**:1–21.
- Alcober O, Martínez R. A new herrerasaurid (Dinosauria, Saurischia) from the Upper Triassic Ischigualasto Formation of Northwestern Argentina. *ZooKeys* 2010;**63**:55–81.
- Ballell A, Rayfield EJ, Benton MJ. Osteological redescription of the Late Triassic sauropodomorph dinosaur *Thecodontosaurus antiquus* based on new material from Tytherington, southwestern England. *Journal of Vertebrate Paleontology* 2020;**40**:e1770774. <https://doi.org/10.1080/02724634.2020.1770774>
- Baron MG, Norman DB, Barrett PM. A new hypothesis of dinosaur relationships and early dinosaur evolution. *Nature* 2017;**543**:501–6. <https://doi.org/10.1038/nature21700>
- Benton MJ. Classification and phylogeny of the diapsid reptiles. *Zoological Journal of the Linnean Society* 1985;**84**:97–164. <https://doi.org/10.1111/j.1096-3642.1985.tb01796.x>
- Benton MJ, Walker AD. *Saltopus*, a dinosauriform from the Upper Triassic of Scotland. *Earth and Environmental Science Transactions of the Royal Society of Edinburgh* 2010;**101**:285–99. <https://doi.org/10.1017/s1755691011020081>
- Bernardi M, Petti F, D’Orazi Porchetti S *et al.* Large tridactyl footprints associated with a diverse ichnofauna from the Carnian of the Southern Alps. *New Mexico Museum of Natural History and Science, Bulletin* 2013;**61**:48–53.

- Bernardi M, Klein H, Petti FM *et al.* The origin and early radiation of Archosauriforms: integrating the skeletal and footprint record (Carrier D, ed.). *PLoS One* 2015; **10**:e0128449. <https://doi.org/10.1371/journal.pone.0128449>
- Bernardi M, Gianolla P, Petti FM *et al.* Dinosaur diversification linked with the Carnian Pluvial Episode. *Nature Communications* 2018; **9**:1499. <https://doi.org/10.1038/s41467-018-03996-1>
- Bourquin S, Eschard R, Hamouche B. High-resolution sequence stratigraphy of Upper Triassic succession (Carnian–Rhaetian) of the Zarzaitine outcrops (Algeria): a model of fluvio-lacustrine deposits. *Journal of African Earth Sciences* 2010; **58**:365–86. <https://doi.org/10.1016/j.jafrearsci.2010.04.003>
- Broom R. Note on *Mesosuchus browni*, Watson, and on a new South African Triassic pseudosuchian (*Euparkeria capensis*). *Records of the Albany Museum* 1913; **2**:394–6.
- Browne J. A science of empire: British biogeography before Darwin. *Revue D'histoire des Sciences* 1992; **45**:453–75. <https://doi.org/10.3406/rhs.1992.4244>
- Brusatte SL, Niedzwiedzki G, Butler RJ. Footprints pull origin and diversification of dinosaur stem lineage deep into Early Triassic. *Proceedings Biological Sciences* 2011; **278**:1107–13. <https://doi.org/10.1098/rspb.2010.1746>
- de Buffrénil V, de Ricqlès AJ, Zylberberg L *et al.* *Vertebrate Skeletal Histology and Paleohistology*. CRC Press, Boca Raton, FL, USA, 2021.
- Button DJ, Lloyd GT, Ezcurra MD *et al.* Mass extinctions drove increased global faunal cosmopolitanism on the supercontinent Pangaea. *Nature Communications* 2017; **8**:733. <https://doi.org/10.1038/s41467-017-00827-7>
- Cabreira S, Schultz C, Bittencourt J *et al.* New stem-sauropodomorph (Dinosauria, Saurischia) from the Triassic of Brazil. *Die Naturwissenschaften* 2011; **98**:1035–40.
- Cabreira SF, Kellner AWA, Dias-da-Silva S *et al.* A unique Late Triassic Dinosauriform assemblage reveals dinosaur ancestral anatomy and diet. *Current Biology* 2016; **26**:3090–5.
- Cau A. The assembly of the avian body plan: a 160-million-year long process. *Bollettino Della Societa Paleontologica Italiana* 2018; **57**:1–25.
- Cheng SJ, Gaynor KM, Moore AC *et al.* Championing inclusive terminology in ecology and evolution. *Trends in Ecology & Evolution* 2023; **38**:381–4. <https://doi.org/10.1016/j.tree.2022.12.011>
- Cohen KM, Finney SC, Gibbard PL *et al.* The ICS international chronostratigraphic chart. *International Commission on Stratigraphy* 2013; **Episodes** **36**:199–204.
- Colombi C, Martínez RN, Césari SN *et al.* A high-precision U–Pb zircon age constraints the timing of the faunistic and palynofloristic events of the Carnian Ischigualasto Formation, San Juan, Argentina. *Journal of South American Earth Sciences* 2021; **111**:103433. <https://doi.org/10.1016/j.jsames.2021.103433>
- Condon DJ, Schoene B, McLean NM *et al.* Metrology and traceability of U–Pb isotope dilution geochronology (EARTHTIME Tracer Calibration Part I). *Geochimica et Cosmochimica Acta* 2015; **164**:464–80. <https://doi.org/10.1016/j.gca.2015.05.026>
- Dal Corso J, Bernardi M, Sun Y *et al.* Extinction and dawn of the modern world in the Carnian (Late Triassic). *Science Advances* 2020; **6**:eaba0099. <https://www.science.org/doi/10.1126/sciadv.aba0099>
- Dawley RM, Zawiskie JM, Cosgriff JW. A raiusuchid thecodont from the Upper Triassic Popo Agie Formation of Wyoming. *Journal of Paleontology* 1979; **53**:1428–31.
- Desojo JB, Fiorelli LE, Ezcurra MD *et al.* The Late Triassic Ischigualasto Formation at Cerro Las Lajas (La Rioja, Argentina): fossil tetrapods, high-resolution chronostratigraphy, and faunal correlations. *Scientific Reports* 2020; **10**:12782.
- Dubiel RF. Triassic deposystems, paleogeography, and paleoclimate of the western interior. In: Caputo MV, Peterson JA, Franczyk KJ (eds), *Mesozoic Systems of the Rocky Mountain Region, USA*. Denver: Rocky Mountain Section SEPM, Denver, Colorado, USA, 1994, 133–68.
- Dunne EM, Farnsworth A, Greene SE *et al.* Climatic drivers of latitudinal variation in Late Triassic tetrapod diversity. *Palaeontology* 2021; **64**:101–17. <https://doi.org/10.1111/pala.12514>
- Dunne EM, Farnsworth A, Benson RBJ *et al.* Climatic controls on the ecological ascendancy of dinosaurs. *Current Biology: CB* 2023; **33**:206–14.e4. <https://doi.org/10.1016/j.cub.2022.11.064>
- Dzik J. A beaked herbivorous archosaur with dinosaur affinities from the early Late Triassic of Poland. *Journal of Vertebrate Paleontology* 2003; **23**:556–74. <https://doi.org/10.1671/a1097>
- Edgar KM, Haller L, Cashmore DD *et al.* Stratigraphic and geographic distribution of dinosaur tracks in the UK. *Journal of the Geological Society* 2023; **180**:jgs2023–003.
- Endersby J. *Imperial Nature: Joseph Hooker and the Practices of Victorian Science*, Paperback edn. Chicago: University of Chicago Press, 2010.
- Ezcurra MD. A new early coelophysoid neotheropod from the Late Triassic of northwestern Argentina. *Ameghiniana* 2017; **54**:506. <https://doi.org/10.5710/amgh.04.08.2017.3100>
- Ezcurra MD, Brusatte SL. Taxonomic and phylogenetic reassessment of the early neotheropod dinosaur *Camposaurus arizonensis* from the Late Triassic of North America. *Palaeontology* 2011; **54**:763–72. <https://doi.org/10.1111/j.1475-4983.2011.01069.x>
- Ezcurra MD, Nesbitt SJ, Bronzati M *et al.* Enigmatic dinosaur precursors bridge the gap to the origin of Pterosauria. *Nature* 2020a; **588**:445–9. <https://doi.org/10.1038/s41586-020-3011-4>
- Ezcurra MD, Nesbitt SJ, Fiorelli LE *et al.* New specimen sheds light on the anatomy and taxonomy of the early Late Triassic Dinosauriforms from the Chañares formation, NW Argentina. *Anatomical Record (Hoboken, N. J.: 2007)* 2020b; **303**:1393–438. <https://doi.org/10.1002/ar.24243>
- Ezcurra MD, Müller RT, Novas FE *et al.* Osteology of the sauropodomorph dinosaur *Jaklapallisaurus asymmetricus* from the Late Triassic of central India. *The Anatomical Record* 2023; **307**:1093–112. <https://doi.org/10.1002/ar.25359>
- Farlow JO, Schachner ER, Sarrazin JC *et al.* Pedal proportions of *Poposaurus gracilis*: convergence and divergence in the feet of archosaurs. *Anatomical Record (Hoboken, N.J.: 2007)* 2014; **297**:1022–46. <https://doi.org/10.1002/ar.22863>
- Ferigolo J, Langer M. A Late Triassic dinosauriform from south Brazil and the origin of the ornithischian predeontary bone. *Historical Biology* 2007; **19**:23–33. <https://doi.org/10.1080/08912960600845767>
- Fitch AJ, Lovelace DM, Stocker MR. The oldest dinosaur from the northern hemisphere and the origins of Theropoda. *Journal of Vertebrate Paleontology, Program and Abstracts* 2020:140–1.
- Fitch AJ, Haas M, C'Hair W *et al.* A new rhynchosaur taxon from the Popo Agie Formation, WY: implications for a Northern Pangean Early–Late Triassic (Carnian) fauna. *Diversity* 2023; **15**:544. <https://doi.org/10.3390/d15040544>
- Foffa D, Whiteside DI, Viegas PA *et al.* Vertebrates from the Late Triassic *Thecodontosaurus*-bearing rocks of Durdham Down, Clifton (Bristol, UK). *Proceedings of the Geologists' Association* 2014; **125**:317–28. <https://doi.org/10.1016/j.jgeola.2014.02.002>
- Fonseca AO, Reid IJ, Venner A *et al.* A comprehensive phylogenetic analysis on early ornithischian evolution. *Journal of Systematic Palaeontology* 2024; **22**:2346577.
- Francillon-Vieillot H, De Buffrénil V, Castanet J *et al.* 1990. Microstructure and mineralization of vertebrate skeletal tissues. In: Carter JG (ed.), *Short Courses in Geology*. NY: Van Nostrand Reinhold, 175–234.
- Galton PM. On the anatomy and relationships of *Efraasia diagnostica* (Huene) n. gen., a prosauropod dinosaur (Reptilia: Saurischia) from the Upper Triassic of Germany. *Paläontologische Zeitschrift* 1973; **47**:229–55. <https://doi.org/10.1007/bf02985709>
- Galton P, Kermack D. The anatomy of *Pantydraco caducus*, a very basal sauropodomorph dinosaur from the Rhaetian (Upper Triassic) of South Wales UK. *Revue de Paleobiologie* 2010; **29**:341–404.
- Gand G, Demathieu G. Les pistes dinosauroïdes du Trias moyen français: interprétation et réévaluation de la nomenclature. *Geobios* 2005; **38**:725–49. <https://doi.org/10.1016/j.geobios.2005.04.001>
- García MS, Cabreira SF, da Silva LR *et al.* A saurischian (Archosauria, Dinosauria) ilium from the Upper Triassic of southern Brazil and the rise of Herrerasauria. *The Anatomical Record* 2023; **307**:1011–24. <https://doi.org/10.1002/ar.25342>
- Gauthier J. Saurischian monophyly and the origin of birds. *Memoirs of the California Academy of Sciences* 1986; **8**:1–55.

- Gerstenberger H, Haase G. A highly effective emitter substance for mass spectrometric Pb isotope ratio determinations. *Chemical Geology* 1997;136:309–12. [https://doi.org/10.1016/S0009-2541\(96\)00033-2](https://doi.org/10.1016/S0009-2541(96)00033-2)
- Geyer G, Kelber KP. Spinicaudata ('Conchostraca', Crustacea) from the Middle Keuper (Upper Triassic) of the southern Germanic Basin, with a review of Carnian–Norian taxa and suggested biozones. *PalZ* 2018;92:1–34.
- Gillman LN, Wright SD. Restoring indigenous names in taxonomy. *Communications Biology* 2020;3:1–3.
- Goloboff PA, Catalano SA. TNT version 1.5, including a full implementation of phylogenetic morphometrics. *Cladistics* 2016;32:221–38. <https://doi.org/10.1111/cla.12160>
- Griffin CT, Bano LS, Turner AH *et al.* Integrating gross morphology and bone histology to assess skeletal maturity in early dinosaurs: new insights from *Dromomeron* (Archosauria: Dinosauria). *PeerJ* 2019;7:e6331. <https://doi.org/10.7717/peerj.6331>
- Griffin CT, Wynd BM, Munyikwa D *et al.* Africa's oldest dinosaurs reveal early suppression of dinosaur distribution. *Nature* 2022;609:313–9. <https://doi.org/10.1038/s41586-022-05133-x>
- Guedes P, Alves-Martins F, Arribas JM *et al.* Eponyms have no place in 21st-century biological nomenclature. *Nature Ecology & Evolution* 2023;7:1157–60. <https://doi.org/10.1038/s41559-023-02022-y>
- Hartman S, Mortimer M, Wahl WR *et al.* A new paravian dinosaur from the Late Jurassic of North America supports a late acquisition of avian flight. *PeerJ* 2019;7:e7247. <https://doi.org/10.7717/peerj.7247>
- Hartman SA, Lovelace DM, Linzmeier BJ *et al.* Mechanistic thermal modeling of Late Triassic terrestrial amniotes predicts biogeographic distribution. *Diversity* 2022;14:973. <https://doi.org/10.3390/d14110973>
- Hasiotis ST. Continental ichnology: fundamental processes and controls on trace fossil distribution. In: Miller III W (ed.), *Trace Fossils*. Elsevier, Kidlington, Oxford, UK, 2007, 268–84.
- Haslett J, Parnell A. A simple monotone process with application to radiocarbon-dated depth chronologies. *Journal of the Royal Statistical Society Series C: Applied Statistics* 2008;57:399–418. <https://doi.org/10.1111/j.1467-9876.2008.00623.x>
- Haubold H, Klein H. The dinosaurid trackways *Parachirotherium–Atripus–Grallator* from the lower Middle Keuper (Upper Triassic: Ladinian, Carnian, ?Norian) of Frankonia (Germany). *Hallesches Jahrbuch für Geowissenschaften* 2000;1–22.
- Haubold H, Klein H. Chirotherians and Grallatorids from lower through Upper Triassic deposits in Central Europe and the origin of dinosaurs. *Hallesches Jahrbuch für Geowissenschaften* 2002;24:1–22.
- Hiesh J, Condon DJ, McLean N *et al.* ²³⁸U/²³⁵U systematics in terrestrial uranium-bearing minerals. *Science* 2012;335:1610–4. <https://doi.org/10.1126/science.1215507>
- High LR, Picard MD. Rock units and revised nomenclature Chugwater Group (Triassic), Western Wyoming. *The Mountain Geologist* 1967;4:73–81.
- Huelsenbeck JP, Ronquist F. MRBAYES: Bayesian inference of phylogenetic trees. *Bioinformatics* 2001;17:754–5. <https://doi.org/10.1093/bioinformatics/17.8.754>
- von Huene FR. *Die Dinosaurier der Europäischen Triasformation mit Berücksichtigung der Ausereuropäischen Vorkommnisse* (part). *Geologie und Paläontologie Abhandlungen* 1908;6:345–419.
- von Huene F. Ein primitiver Dinosaurier aus der mittleren Trias von Elgin. *Geologische und Paläontologische Abhandlungen, Neue Folge* 1910;8:315–22.
- Irmis RB, Mundil R, Martz JW *et al.* High-resolution U–Pb ages from the Upper Triassic Chinle formation (New Mexico, USA) support a diachronous rise of dinosaurs. *Earth and Planetary Science Letters* 2011;309:258–67. <https://doi.org/10.1016/j.epsl.2011.07.015>
- Jaffey AH, Flynn KF, Glendenin LE *et al.* Precision measurement of half-lives and specific activities of ²³⁵U and ²³⁸U. *Physical Review C* 1971;4:1889–906. <https://doi.org/10.1103/physrevc.4.1889>
- Johnson EA. 1993. *Depositional History of Triassic Rocks in the Area of the Powder River Basin, Northeastern Wyoming and Southeastern Montana*, U.S. Geological Survey Bulletin, 1917: P1-P30.
- Jones ME, Anderson C, Hipsley CA *et al.* Integration of molecules and new fossils supports a Triassic origin for Lepidosauria (lizards, snakes, and tuatara). *BMC Evolutionary Biology* 2013;13:208–21. <https://doi.org/10.1186/1471-2148-13-208>
- Jost L, Yanez-Muñoz MH, Brito J *et al.* Eponyms are important tools for biologists in the Global South. *Nature Ecology & Evolution* 2023;7:1164–5. <https://doi.org/10.1038/s41559-023-02102-z>
- Kammerer CF, Nesbitt SJ, Shubin NH. The first silesaurid dinosauriform from the Late Triassic of Morocco. *Acta Palaeontologica Polonica* 2012;57:277–84. <https://doi.org/10.4202/app.2011.0015>
- Kammerer CF, Butler RJ, Bandyopadhyay S *et al.* Relationships of the Indian phytosaur *Parasuchus hislopi* Lydekker, 1885. *Papers in Palaeontology* 2016;2:1–23. <https://doi.org/10.1002/spp2.1022>
- Kent DV, Clemmensen LB. Northward dispersal of dinosaurs from Gondwana to Greenland at the mid-Norian (215–212 Ma, Late Triassic) dip in atmospheric pCO₂. *Proceedings of the National Academy of Sciences* 2021;118:e2020778118.
- Khalifa MA. Triassic–Jurassic boundary on the southern margin of Tethys: implications of facies, tectonics and volcanism. *New Mexico Museum of Natural History and Science Bulletin* 2007;41:110–9.
- Kirmse JPS, Benton MJ, Hildebrandt C *et al.* A Coelophysoidea (Dinosauria, Theropoda) femur from the Tytherington fissures (Rhaetian, Late Triassic), Bristol, UK. *Proceedings of the Geologists' Association* 2023;134:562–72.
- Kischlat EE, Lucas SG. A phytosaur from the Upper Triassic of Brazil. *Journal of Vertebrate Paleontology* 2003;23:464–7. [https://doi.org/10.1671/0272-4634\(2003\)023\[0464:apftut\]2.0.co;2](https://doi.org/10.1671/0272-4634(2003)023[0464:apftut]2.0.co;2)
- Klein H, Lucas SG. The Triassic tetrapod footprint record. *New Mexico Museum of Natural History and Science, Bulletin* 2021;83:1–194.
- Klein H, Voigt S, Saber H *et al.* First occurrence of a Middle Triassic tetrapod ichnofauna from the Argana Basin (Western High Atlas, Morocco). *Palaeogeography, Palaeoclimatology, Palaeoecology* 2011;307:218–31. <https://doi.org/10.1016/j.palaeo.2011.05.021>
- Kozur HW, Weems RE. The biostratigraphic importance of conchostracans in the continental Triassic of the northern hemisphere. *Geological Society, London, Special Publications* 2010;334:315–417. <https://doi.org/10.1144/sp334.13>
- Krogh TE. A low-contamination method for hydrothermal decomposition of zircon and extraction of U and Pb for isotopic age determinations. *Geochimica et Cosmochimica Acta* 1973;37:485–94. [https://doi.org/10.1016/0016-7037\(73\)90213-5](https://doi.org/10.1016/0016-7037(73)90213-5)
- Krone IW, Magoulick KM, Yohler RM. All the Earth will not remember: how geographic gaps structure the record of diversity and extinction. *Paleobiology* 2024;50:214–25. <https://doi.org/10.1017/pab.2023.34>
- Kufner AM, Lovelace DM. Taphonomy of two Late Triassic stereospondyl mass death assemblages from the Popo Agie Formation (Fremont County, Wyoming). *Journal of Vertebrate Paleontology, Program and Abstracts* 2018:162.
- Kufner AM, Blomberg OH, Gonzales HM *et al.* Specimen-level assessment of ontogeny and phylogeny of North American metoposaurids (Tetrapoda, Temnospondyli). *Journal of Vertebrate Paleontology, Program and Abstracts* 2023:255.
- Langer MC, Ferigolo J. The Late Triassic dinosauriform *Sacisaurus agudoensis* (Caturrita Formation; Rio Grande do Sul, Brazil): anatomy and affinities. *Geological Society, London, Special Publications* 2013;379:353–92. <https://doi.org/10.1144/sp379.16>
- Langer MC, Abdala F, Richter M *et al.* A sauropodomorph dinosaur from the Upper Triassic (Carnian) of southern Brazil. *Comptes Rendus de l'Académie des Sciences—Series IIA—Earth and Planetary Science* 1999;329:511–7. [https://doi.org/10.1016/S1251-8050\(00\)80025-7](https://doi.org/10.1016/S1251-8050(00)80025-7)
- Langer MC, Ezcurra MD, Bittencourt JS *et al.* The origin and early evolution of dinosaurs. *Biological Reviews of the Cambridge Philosophical Society* 2010;85:55–110. <https://doi.org/10.1111/j.1469-185X.2009.00094.x>
- Langer MC, Nesbitt SJ, Bittencourt JS *et al.* Non-dinosaurian Dinosauriforms. In: Nesbitt S, Desojo JB, Irmis RB (ed.), *Geological Society, London, Special Publications* 2013;379:157–86. <https://doi.org/10.1144/sp379.9>

- Langer MC, Ezcurra MD, Rauhut OWM *et al.* Untangling the dinosaur family tree. *Nature* 2017;**551**:E1–3. <https://doi.org/10.1038/nature24011>
- Langer MC, Ramezani J, Da Rosa AAS. U–Pb age constraints on dinosaur rise from south Brazil. *Gondwana Research* 2018;**57**:133–40.
- Langer MC, McPhee BW, Marsola JCA *et al.* Anatomy of the dinosaur *Pampadromaeus barberenai* (Saurischia—Sauropodomorpha) from the Late Triassic Santa Maria Formation of southern Brazil. *PLoS One* 2019;**14**:e0212543.
- Leal LA, Azevedo SK, Kellner AWA *et al.* A new early dinosaur (Sauropodomorpha) from the Caturrita Formation (Late Triassic), Paran Basin, Brazil. *Zootaxa* 2004;**690**:1–24.
- Lee MSY, Baron MG, Norman DB *et al.* Dynamic biogeographic models and dinosaur origins. *Earth and Environmental Science Transactions of The Royal Society of Edinburgh* 2018;**109**:325–32. <https://doi.org/10.1017/s1755691018000920>
- Liboiron M. Decolonizing geoscience requires more than equity and inclusion. *Nature Geoscience* 2021;**14**:876–7. <https://doi.org/10.1038/s41561-021-00861-7>
- Lichtig AJ, Lucas SG, Klein H *et al.* Triassic turtle tracks and the origin of turtles. *Historical Biology* 2018;**30**:1112–22. <https://doi.org/10.1080/08912963.2017.1339037>
- Lockley M, Lucas S. *Evazoum gatewayensis* a new Late Triassic archosaurian ichnospecies from Colorado: implications for footprints in the ichnofamily Otozoidae. *New Mexico Museum of Natural History and Science Bulletin* 2013;**61**:345–53.
- Lockley MG, Lallensack JN, Sciscio L *et al.* The early Mesozoic saurischian trackways *Evazoum* and *Otozoum*: implications for ‘prosauropod’ (basal sauropodomorph) gaits. *Historical Biology* 2024;**36**:406–24.
- Long R, Murry P. Late Triassic (Carnian and Norian) Tetrapods from the Southwestern United States cover. *New Mexico Museum of Natural History and Science Bulletin* 1995;**4**:1–254.
- Lovelace DM. Triassic macrostratigraphy of the western United States and the ichnology, paleoecology, and paleoenvironments of the Early and Middle Triassic of the Chugwater Group, Wyoming. Unpublished doctoral thesis, University of Wisconsin-Madison, 2012.
- Lovelace DM, Doebbert AC. A new age constraint for the Early Triassic Alcova Limestone (Chugwater Group), Wyoming. *Palaeogeography, Palaeoclimatology, Palaeoecology* 2015;**424**:1–5. <https://doi.org/10.1016/j.palaeo.2015.02.009>
- Lovelace DM, Lovelace SD. Paleoenvironments and paleoecology of a lower Triassic invertebrate and vertebrate ichnoassemblage from the red peak formation (Chugwater Group), central Wyoming. *PALAIOS* 2012;**27**:636–57. <https://doi.org/10.2110/palo.2012.p12-011r>
- Lovelace DM, Hartman SA, Mathewson PD *et al.* Modeling dragons: using linked mechanistic physiological and microclimate models to explore environmental, physiological, and morphological constraints on the early evolution of dinosaurs (Joger U, ed.). *PLoS One* 2020;**15**:e0223872. <https://doi.org/10.1371/journal.pone.0223872>
- Lovelace DM, Fitch AJ, Schwartz D, *et al.* Concurrence of Late Triassic lithostratigraphic, radioisotopic, and biostratigraphic data support a Carnian age for the Popo Agie Formation (Chugwater Group), Wyoming, USA. *GSA Bulletin* 2024;**136**:2305–24. <https://doi.org/10.1130/B36807.1>
- Macdonald FA, Schmitz MD, Strauss JV *et al.* Cryogenian of Yukon. *Precambrian Research* 2018;**319**:114–43. <https://doi.org/10.1016/j.precamres.2017.08.015>
- Marsh AD, Parker WG, Langer MC *et al.* Redescription of the holotype specimen of *Chindesaurus bryansmalli* Long and Murry, 1995 (Dinosauria, Theropoda), from Petrified Forest National Park, Arizona. *Journal of Vertebrate Paleontology* 2019;**39**:e1645682. <https://doi.org/10.1080/02724634.2019.1645682>
- Marsicano CA, Domnanovich NS, Mancuso AC. Dinosaur origins: evidence from the footprint record. *Historical Biology* 2007;**19**:83–91. <https://doi.org/10.1080/08912960600866920>
- Marsicano CA, Irmis RB, Mancuso AC *et al.* The precise temporal calibration of dinosaur origins. *Proceedings of the National Academy of Sciences of the United States of America* 2016;**113**:509–13. <https://doi.org/10.1073/pnas.1512541112>
- Marsola JCA, Bittencourt JS, Butler RJ *et al.* A new dinosaur with theropod affinities from the Late Triassic Santa Maria Formation, south Brazil. *Journal of Vertebrate Paleontology* 2018;**38**:e1531878. <https://doi.org/10.1080/02724634.2018.1531878>
- Martinez RN, Alcober OA. A basal sauropodomorph (Dinosauria: Saurischia) from the Ischigualasto Formation (Triassic, Carnian) and the early evolution of Sauropodomorpha. *PLoS One* 2009;**4**:e4397. <https://doi.org/10.1371/journal.pone.0004397>
- Martinez RN, Sereno PC, Alcober OA *et al.* A basal dinosaur from the dawn of the dinosaur era in southwestern Pangaea. *Science* 2011;**331**:206–10. <https://doi.org/10.1126/science.1198467>
- Martínez RN, Apaldetti C, Alcober OA *et al.* Vertebrate succession in the Ischigualasto Formation. *Journal of Vertebrate Paleontology* 2012;**32**:10–30. <https://doi.org/10.1080/02724634.2013.818546>
- Martz JW, Parker WG. 2017. Revised formulation of the Late Triassic land vertebrate ‘Faunachrons’ of Western North America. In: Ziegler KE, Parker WJ (ed.), *Terrestrial Depositional Systems*. Elsevier: Amsterdam, Netherlands, 39–125.
- Martz JW, Small BJ. Non-dinosaurian dinosauriforms from the Chinle Formation (Upper Triassic) of the Eagle Basin, northern Colorado: *Dromomeron romeri* (Lagerpetidae) and a new taxon, *Kwanasaurus williamparkeri* (Silesauridae). *PeerJ* 2019;**7**:e7551. <https://doi.org/10.7717/peerj.7551>
- Mattinson JM. Zircon U–Pb chemical abrasion (‘CA-TIMS’) method: combined annealing and multi-step partial dissolution analysis for improved precision and accuracy of zircon ages. *Chemical Geology* 2005;**220**:47–66. <https://doi.org/10.1016/j.chemgeo.2005.03.011>
- Menning M, Hendrich A; Deutsche Union der Geowissenschaften (eds), *Stratigraphische Tabelle von Deutschland 2016: STDK 2022*. Potsdam: GeoForschungszentrum, 2022.
- Mestriner G, Marsola JCA, Nesbitt SJ *et al.* Anatomy and phylogenetic affinities of a new silesaurid assemblage from the Carnian beds of South Brazil. *Journal of Vertebrate Paleontology* 2023;**43**:e2232426. <https://doi.org/10.1080/02724634.2023.2232426>
- Milroy P, Wright VP, Simms MJ. Dryland continental mudstones: deciphering environmental changes in problematic mudstones from the Upper Triassic (Carnian to Norian) Mercia Mudstone Group, South-West Britain. *Sedimentology* 2019;**66**:2557–89. <https://doi.org/10.1111/sed.12626>
- Monarrez PM, Zimmt JB, Clement AM *et al.* Our past creates our present: a brief overview of racism and colonialism in Western paleontology. *Paleobiology* 2022;**48**:173–85. <https://doi.org/10.1017/pab.2021.28>
- Moro D, Damke LVS, Müller RT *et al.* An unusually robust specimen attributed to *Buriolestes schultzi* (Dinosauria: Sauropodomorpha) from the Late Triassic of Southern Brazil. *Anatomical Record (Hoboken, N. J.: 2007)* 2024;**307**:1025–59. <https://doi.org/10.1002/ar.25319>
- Müller RT. Astragalar anatomy of an early dinosaur from the Upper Triassic of southern Brazil. *Historical Biology* 2021;**33**:2534–41. <https://doi.org/10.1080/08912963.2020.1814276>
- Müller RT. On the presence and shape of anterolateral scars in the ontogenetic series of femora for two early sauropodomorph dinosaurs from the Upper Triassic of Brazil. *Paleontological Research* 2022;**26**:1–7. <https://doi.org/10.2517/PR200001>
- Müller RT, Garcia MS. A paraphyletic ‘Silesauridae’ as an alternative hypothesis for the initial radiation of ornithischian dinosaurs. *Biology Letters* 2020;**16**:20200417. <https://doi.org/10.1098/rsbl.2020.0417>
- Müller RT, Garcia MS. Oldest dinosauriform from South America and the early radiation of dinosaur precursors in Gondwana. *Gondwana Research* 2022;**107**:42–8. <https://doi.org/10.1016/j.gr.2022.02.010>
- Müller RT, Garcia MS. A new silesaurid from Carnian beds of Brazil fills a gap in the radiation of avian line archosaurs. *Scientific Reports* 2023;**13**:4981. <https://doi.org/10.1038/s41598-023-32057-x>
- Müller RT, Langer MC, Dias-da-Silva S. An exceptionally preserved association of complete dinosaur skeletons reveals the oldest long-necked sauropodomorphs. *Biology Letters* 2018;**14**:20180633. <https://doi.org/10.1098/rsbl.2018.0633>
- Nesbitt SJ. The early evolution of archosaurs: relationships and the origin of major clades. *Bulletin of the American Museum of Natural History* 2011;**352**:1–292. <https://doi.org/10.1206/352.1>

- Nesbitt SJ, Ezcurra MD. The early fossil record of dinosaurs in North America: a new neotheropod from the base of the Upper Triassic Dockum group of Texas. *Acta Palaeontologica Polonica* 2015;**60**:513–26.
- Nesbitt SJ, Sidor CA, Irmis RB *et al.* Ecologically distinct dinosaurian sister group shows early diversification of Ornithodira. *Nature* 2010;**464**:95–8. <https://doi.org/10.1038/nature08718>
- Nesbitt SJ, Langer MC, Ezcurra MD. The anatomy of *Asilisaurus kongwe*, a Dinosauriform from the Lifua member of the Manda beds (Middle Triassic) of Africa. *The Anatomical Record* 2020a;**303**:813–73.
- Nesbitt SJ, Zawiskie JM, Dawley RM. The osteology and phylogenetic position of the loricatan (Archosauria: Pseudosuchia) *Heptasuchus clarki*, from the ?Mid–Upper Triassic, southeastern Big Horn Mountains, Central Wyoming (USA). *PeerJ* 2020b;**8**:e10101. <https://doi.org/10.7717/peerj.10101>
- Nicosia U, Loi M. Triassic footprints from Lericci (La Spezia, Northern Italy). *Ichnos* 2003;**10**:127–40. <https://doi.org/10.1080/10420940390256203>
- Niedźwiedzki G, Szrek P, Narkiewicz K *et al.* Tetrapod trackways from the early Middle Devonian period of Poland. *Nature* 2010;**463**:43–8. <https://doi.org/10.1038/nature08623>
- Norman DB, Baron MG, Garcia MS *et al.* Taxonomic, palaeobiological and evolutionary implications of a phylogenetic hypothesis for Ornithischia (Archosauria: Dinosauria). *Zoological Journal of the Linnean Society* 2022;**196**:1273–309. <https://doi.org/10.1093/zoolinnean/zlac062>
- Novas FE. New information on the systematics and postcranial skeleton of *Herrerasaurus ischigualastensis* (Theropoda: Herrerasauridae) from the Ischigualasto Formation (Upper Triassic) of Argentina. *Journal of Vertebrate Paleontology* 1994;**13**:400–23. <https://doi.org/10.1080/02724634.1994.10011523>
- Novas FE, Ezcurra MD, Chatterjee S *et al.* New dinosaur species from the Upper Triassic Upper Maleri and Lower Dharmaram formations of Central India. *Earth and Environmental Science Transactions of The Royal Society of Edinburgh* 2010;**101**:333–49. <https://doi.org/10.1017/s1755691011020093>
- Novas FE, Agnolin FL, Ezcurra MD *et al.* Review of the fossil record of early dinosaurs from South America, and its phylogenetic implications. *Journal of South American Earth Sciences* 2021;**110**:103341. <https://doi.org/10.1016/j.jsames.2021.103341>
- Olsen PE, Kent DV, Whiteside JH. Implications of the Newark Supergroup-based astrochronology and geomagnetic polarity time scale (Newark-APTS) for the tempo and mode of the early diversification of the Dinosauria. *Earth and Environmental Science Transactions of the Royal Society of Edinburgh* 2010;**101**:201–29. <https://doi.org/10.1017/s1755691011020032>
- Orr MC, Hughes AC, Carvajal OT *et al.* Inclusive and productive ways forward needed for species-naming conventions. *Nature Ecology & Evolution* 2023;**7**:1168–9. <https://doi.org/10.1038/s41559-023-02103-y>
- Padian K, Lamm ET (eds). *Bone Histology of Fossil Tetrapods: Advancing Methods, Analysis, and Interpretation*. Berkeley: University of California Press, 2013.
- Padian K, May C. The earliest dinosaurs. *New Mexico Museum of Natural History and Science Bulletin* 1993;**3**:379–81.
- Palma RL, Heath ACG. Science versus vernacular: should some taxa of animals and plants be renamed according to ‘indigenous’ practices? *Bionomina* 2021;**22**:1–7.
- Peabody FE. *Reptile and Amphibian Trackways from the Lower Triassic Moenkopi Formation of Arizona and Utah*. In: Peabody FE (ed.). University of California Press, Berkeley, California, USA, 1948;**27**:295–468.
- Peacock BR, Sidor CA, Nesbitt SJ *et al.* A new silesaurid from the upper Ntawere Formation of Zambia (Middle Triassic) demonstrates the rapid diversification of Silesauridae (Avmemetatarsalia, Dinosauriformes). *Journal of Vertebrate Paleontology* 2013;**33**:1127–37. <https://doi.org/10.1080/02724634.2013.755991>
- Pethiyagoda R. Policing the scientific lexicon: the new colonialism?. *Megatata* 2023;**10**:20–5.
- Philipp RP, Schultz CL, Kloss HP *et al.* Middle Triassic SW Gondwana paleogeography and sedimentary dispersal revealed by integration of stratigraphy and U-Pb zircon analysis: the Santa Cruz Sequence, Paraná Basin, Brazil. *Journal of South American Earth Sciences* 2018;**88**:216–37.
- Pol D, Otero A, Apaldetti C *et al.* Triassic sauropodomorph dinosaurs from South America: the origin and diversification of dinosaur dominated herbivorous faunas. *Journal of South American Earth Sciences* 2021;**107**:103145. <https://doi.org/10.1016/j.jsames.2020.103145>
- Porchetti SD, Nicosia U, Mietto P *et al.* *Atreipus*-like footprints and their co-occurrence with *Evazoum* from the upper Carnian (Tuvalian) of Trentino-Alto Adige. *Studi trentini di scienze naturali - Acta geologica* 2008;227–287 2008.
- Pretto FA, Müller RT, Moro D *et al.* The oldest South American silesaurid: new remains from the Middle Triassic (Pinheiros-Chiniquá Sequence, *Dinodontosaurus* Assemblage Zone) increase the time range of silesaurid fossil record in southern Brazil. *Journal of South American Earth Sciences* 2022;**120**:104039. <https://doi.org/10.1016/j.jsames.2022.104039>
- Rasmussen C, Mundil R, Irmis RB *et al.* U-Pb zircon geochronology and depositional age models for the Upper Triassic Chinle Formation (Petrified Forest National Park, Arizona, USA): implications for Late Triassic paleoecological and paleoenvironmental change. *GSA Bulletin* 2020;**133**:539–58. <https://doi.org/10.1130/b35485.1>
- Reig OA. La presencia de dinosaurios saurisquios en los ‘Estratos de Ischigualasto’ (Mesotriásico Superior) de las provincias de San Juan y La Rioja (República Argentina). *Ameghiniana* 1963;**3**:3–20.
- Romer AS. The Chañares (Argentina) Triassic reptile fauna. X. Two new but incompletely known long-limbed pseudosuchians. *Breviora* 1971;**378**:3781–10.
- Romer AS. The Chañares (Argentina) Triassic reptile fauna. XIV. *Lewisuchus admixtus* gen. et sp. nov., a further thecodont from the Chañares Beds. *Breviora* 1972;**390**:1–7.
- Ronquist F, Huelsenbeck JP. MrBayes 3: Bayesian phylogenetic inference under mixed models. *Bioinformatics* 2003;**19**:1572–4. <https://doi.org/10.1093/bioinformatics/btg180>
- Rummy P, Rummy JT. Recontextualising the style of naming in nomenclature. *Humanities and Social Sciences Communications* 2021;**8**:1–6.
- Schiebinger LL. *Plants and Empire: Colonial Bioprospecting in the Atlantic World*. Cambridge, MA: Harvard University Press, 2004.
- Schmitz MD, Schoene B. Derivation of isotope ratios, errors, and error correlations for U-Pb geochronology using ²⁰⁵Pb-²³⁵U-(²³³U)-spiked isotope dilution thermal ionization mass spectrometric data. *Geochemistry, Geophysics, Geosystems* 2007;**8**:1–20. <https://doi.org/10.1029/2006GC001492>
- Schultz CL, Martinelli AG, Soares MB *et al.* Triassic faunal successions of the Paraná Basin, southern Brazil. *Journal of South American Earth Sciences* 2020;**104**:102846.
- Sellwood BW, Valdes PJ. Mesozoic climates: general circulation models and the rock record. *Sedimentary Geology* 2006;**190**:269–87. <https://doi.org/10.1016/j.sedgeo.2006.05.013>
- Sereno PC, Arcucci AB. Dinosaurian precursors from the Middle Triassic of Argentina: *Lagerpeton chanarensis*. *Journal of Vertebrate Paleontology* 1994;**13**:385–99. <https://doi.org/10.1080/02724634.1994.10011522>
- Sereno PC, Forster CA, Rogers RR *et al.* Primitive dinosaur skeleton from Argentina and the early evolution of Dinosauria. *Nature* 1993;**361**:64–6. <https://doi.org/10.1038/361064a0>
- Sereno PC, Martínez RN, Alcober OA. Osteology of *Eoraptor lunensis* (Dinosauria, Sauropodomorpha). *Journal of Vertebrate Paleontology* 2012;**32**:83–179. <https://doi.org/10.1080/02724634.2013.820113>
- Shubin NH, Daeschler EB, Jenkins FA. The pectoral fin of *Tiktaalik roseae* and the origin of the tetrapod limb. *Nature* 2006;**440**:764–71. <https://doi.org/10.1038/nature04637>
- Simms MJ, Drost K. Caves, dinosaurs and the Carnian Pluvial Episode: recalibrating Britain’s Triassic karst ‘fissures’. *Palaeogeography, Palaeoclimatology, Palaeoecology* 2024;**638**:112041. <https://doi.org/10.1016/j.palaeo.2024.112041>
- Simms MJ, Ruffell AH. Synchronicity of climatic change and extinctions in the Late Triassic. *Geology* 1989;**17**:265–8. [https://doi.org/10.1130/0091-7613\(1989\)017<0265:soccae>2.3.co;2](https://doi.org/10.1130/0091-7613(1989)017<0265:soccae>2.3.co;2)

- So C, Kufner AM, Pardo JD *et al.* Fossil amphibian offers insights into the interplay between monsoons and amphibian evolution in paleoequatorial Late Triassic systems. *Proceedings of the Royal Society of London. Series B: Biological Sciences* In Press 2024;**291**:20241041. <https://doi.org/10.1098/rspb.2024.1041>
- Spiekman SNF, Ezcurra MD, Butler RJ *et al.* *Pendraig milnerae*, a new small-sized coelophysoid theropod from the Late Triassic of Wales. *Royal Society Open Science* 2021;**8**:210915. <https://doi.org/10.1098/rsos.210915>
- Sues HD, Olsen PE. Stratigraphic and temporal context and faunal diversity of Permian–Jurassic continental tetrapod assemblages from the Fundy rift basin, eastern Canada. *Atlantic Geology* 2015;**51**:139–205. <https://doi.org/10.4138/atlgel.2015.006>
- Sues HD, Fitch AJ, Whatley RL. A new rhynchosaur (Reptilia, Archosauromorpha) from the Upper Triassic of eastern North America. *Journal of Vertebrate Paleontology* 2020;**40**:e1771568. <https://doi.org/10.1080/02724634.2020.1771568>
- Szulc J, Racki G, Jewula K *et al.* How many Upper Triassic bone-bearing levels are there in Upper Silesia (southern Poland)? A critical overview of stratigraphy and facies. *Annales Societatis Geologorum Poloniae* 2015;**85**:587–626. <https://doi.org/10.14241/asgp.2015.037>
- Tourani A, Benaouiss N, De La Horra R *et al.* Characterization of the Carnian Pluvial Episode in the Argana Basin (Western High Atlas, Morocco): an approach based on sedimentology, clay mineralogy and palaeosols. *Palaeogeography, Palaeoclimatology, Palaeoecology* 2023;**627**:111720. <https://doi.org/10.1016/j.palaeo.2023.111720>
- Trayler RB, Schmitz MD, Cuitiño JI *et al.* An improved approach to age-modeling in deep time: implications for the Santa Cruz Formation, Argentina. *GSA Bulletin* 2020;**132**:233–44.
- Whiteside JH, Lindström S, Irmis RB *et al.* Extreme ecosystem instability suppressed tropical dinosaur dominance for 30 million years. *Proceedings of the National Academy of Sciences of the United States of America* 2015;**112**:7909–13. <https://doi.org/10.1073/pnas.1505252112>
- Whiteside DI, Duffin CJ, Gill PG *et al.* The Late Triassic and Early Jurassic fissure faunas from Bristol and South Wales: stratigraphy and setting. *Palaeontologia Polonica* 2016;**67**:257–87.
- Wilder BT, O'Meara C, Monti L *et al.* The importance of indigenous knowledge in curbing the loss of language and biodiversity. *BioScience* 2016;**66**:499–509. <https://doi.org/10.1093/biosci/biw026>
- Yates AM. The species taxonomy of the sauropodomorph dinosaurs from the Löwenstein Formation (Norian, Late Triassic) of Germany. *Palaeontology* 2003;**46**:317–37. <https://doi.org/10.1111/j.0031-0239.2003.00301.x>
- Yates AM. The first complete skull of the Triassic dinosaur *Melanorosaurus* Houghton (Sauropodomorpha: Anchisauria). *Special Papers in Palaeontology* 2007;**77**:245–60.
- Ye S, Peters SE. Bedrock geological map predictions for Phanerozoic fossil occurrences. *Paleobiology* 2023;**49**:394–413. <https://doi.org/10.1017/pab.2022.46>
- Zeh A, Franz M, Obst K. Zircon of Triassic age in the Stuttgart Formation (Schilfsandstein)—witness of tephra fallout in the Central European basin and new constraints on the mid-Carnian Episode. *Frontiers in Earth Science* 2021;**9**:778820. <https://doi.org/10.3389/feart.2021.778820>
- Zouheir T, Hminna A, Klein H *et al.* Unusual archosaur trackway and associated tetrapod ichnofauna from Irohalene member (Timezgadiouine formation, late Triassic, Carnian) of the Argana Basin, Western High Atlas, Morocco. *Historical Biology* 2020;**32**:589–601. <https://doi.org/10.1080/08912963.2018.1513506>